A Biophysical Study of Integral Membrane Protein Folding[†]

John F. Hunt,[‡,§] Thomas N. Earnest,[||,⊥] Olaf Bousché,[||] Krishna Kalghatgi,[▽,#] Karlyne Reilly,[‡,○] Csaba Horváth,[▽] Kenneth J. Rothschild,[||] and Donald M. Engelman*[,‡]

Department of Molecular Biophysics and Biochemistry and Department of Chemical Engineering, Yale University, New Haven, Connecticut 06511, and Department of Physics and Molecular Biophysics Laboratory, Boston University, Boston, Massachusetts 02215

Received January 23, 1997; Revised Manuscript Received September 3, 1997[⊗]

ABSTRACT: In order to characterize the thermodynamic constraints on the process of integral membrane protein folding and assembly, we have conducted a biophysical dissection of the structure of bacteriorhodopsin (BR), a prototypical α-helical integral membrane protein. Seven polypeptides were synthesized, corresponding to each of the seven transmembrane α-helices in BR, and the structure of each individual polypeptide was characterized in reconstituted phospholipid vesicles. Five of the seven polypeptides form stable transmembrane α-helices in isolation from the remainder of the tertiary structure of BR. However, using our reconstitution protocols, the polypeptide corresponding to the F helix in BR does not form any stable secondary structure in reconstituted vesicles, and the polypeptide corresponding to the G helix forms a hyperstable *β*-sheet structure with its strands oriented perpendicular to the plane of the membrane. [The polypeptide corresponding to the C helix spontaneously equilibrates in a pH-dependent manner between a transmembrane α-helical conformation, a peripherally bound nonhelical conformation, and a fully water soluble conformation; the conformational properties of this polypeptide are the subject of the accompanying paper: Hunt et al. (1997) *Biochemistry 36*, 15177−15192.] Our observations suggest that the folding of α-helical integral membrane proteins may proceed spontaneously. However, the preference for a non-native conformation exhibited by two of the polypeptides suggests that the formation of some transmembrane substructures could require external constraints such as the links between the helices, interactions with the rest of the protein, or the involvement of cellular chaperones or translocases. Our results also suggest a strategy for improving the thermodynamic stability of α-helical integral membrane proteins, a goal that could facilitate attempts to overexpress and/or refold them.

According to the Anfinsen paradigm, all of the information necessary for the folding of a protein is contained in its linear sequence of amino acids (Anfinsen, 1973). Thirty-five years of research support the validity of this inference with respect to the folding of water-soluble proteins in that they all seem to be capable of folding to the native state on their own (Fersht, 1993; Dobson, 1994; Ptitsyn, 1995). However, the efficiency of this process can be poor, especially in the crowded molecular environment inside living cells, and research during the last ten years has established that a large class of molecular chaperone proteins has evolved to control and assist the folding of water-soluble proteins *in vivo* (Hartl, 1996; Ellis, 1994; Georgopoulos & Welch, 1993). Although it is generally assumed that these same basic principles and chaperone systems are involved in the folding of integral membrane proteins (IMP's),[1] *i.e.* proteins that reside in the heterogeneous chemical microenvironment of the phospholipid bilayer, detailed knowledge in this area remains in a comparatively primitive state. The spontaneous refolding of IMP's has been demonstrated in principle (Huang et al., 1981; Popot et al., 1987; Surrey & Jahnig, 1992; Kleinschmidt & Tamm, 1996), although for a very small number of proteins, and there are a few well-characterized examples establishing the participation of specific molecular chaperones in the folding and/or assembly of some individual IMP's (Kumamoto, 1991; Baker et al., 1994; Ora & Helenius, 1995). However, the generality of these results remains to be established. And, given the small number of systems that have been characterized phenomenologically, very limited mechanistic data are available concerning the structural/thermodynamic pathway of IMP folding (von Heijne, 1994; von Heijne & Blomberg, 1979; Blobel, 1980; Engelman & Steitz, 1981; Wickner, 1980).

In the meantime, it has been proposed that the folding pathway could be particularly simple for IMP's with exclusively α-helical transmembrane (TM) structure (Engelman & Steitz, 1981; Popot & Engelman, 1990). Hydr-

[†] This work was supported by grants from the NIH (GM22778) and the NSF (MCB9406983) to D.M.E. and grants from the NIH-NEI (EY05499) and the NSF (MCB9419059) to K.J.R.

* Corresponding author.

[‡] Department of Molecular Biophysics and Biochemistry, Yale University.

[▽] Department of Chemical Engineering, Yale University.

[||] Department of Physics and Molecular Biophysics Laboratory, Boston University.

[§] Present address: Department of Biological Sciences, Columbia University, New York, NY 10027. E-mail: hunt@sid.bio.columbia.edu.

[⊥] Present address: Physical Biosciences Division, Macromolecular Crystallography Facility at the Advanced Light Source, Lawrence Berkeley National Lab, Berkeley, CA 94720.

[#] Present address: Millenium Pharma, Cambridge, MA 02139.

[○] Present address: Cancer Research Center at MIT, Cambridge, MA 02139.

[⊗] Abstract published in *Advance ACS Abstracts,* November 1, 1997.

[1] Abbreviations: BR, bacteriorhodopsin; CD, circular dichroism; CHAPS, 3-[(3-cholamidopropyl)dimethylammonio]-1-propanesulfonate; FAB, fast atom bombardment; FTIR, Fourier transform infrared spectroscopy; IMP, integral membrane protein; MS, mass spectrometry; PMSF, phenylmethylsulfonyl fluoride; TFA, trifluoroacetic acid; THF, tetrahydrofuran; TM, transmembrane.

S0006-2960(97)00146-3 CCC: $14.00

opathy algorithms identify putative TM α-helices in the primary sequence of an IMP by scanning it for regions that are long enough and hydrophobic enough to span a phospholipid bilayer in an α-helical conformation (von Heijne, 1980; Kyte & Doolittle, 1982; Engelman et al., 1986); these algorithms are believed to be quite reliable and have proven to be correct for the small set of α-helical IMP's where structure has been characterized at high resolution (Engelman et al., 1986). One hydropathy algorithm estimates the free energy of transferring each 20-residue segment of the protein from water into a phospholipid bilayer in an α-helical conformation (Engelman et al., 1986). The magnitude of the free energy of insertion estimated in this way is very large, with values ≤ -15 kcal/mol calculated for the experimentally observed structures. Because this estimate is made for a single, isolated TM α-helix, it suggests that these helices should be thermodynamically stable in the TM configuration, even in the absence of any other structural interactions. On this basis, the folding of polytopic α-helical IMP's (*i.e.* proteins with more than one TM α-helix) could proceed by a simple, two-step pathway in which all of the individual α-helices are stably inserted into the phospholipid bilayer in the first step followed by their association within the plane of the bilayer to form the final tertiary structure in a second, mechanistically independent step (Popot & Engelman, 1990).

If this two-step model were correct in detail, the folding of polytopic α-helical IMP's would be expected to proceed efficiently both *in vivo* and *in vitro*. Moreover, these proteins would be expected to be conformationally robust once inserted into a phospholipid bilayer because transient unfolding fluctuations would simply return the protein to the intermediate state comprising the individually stable TM α-helices. However, both of these expectations stand in contrast to the common biochemical experience with polytopic α-helical IMP's because most of them do not efficiently re-fold to the native state once denatured and many of them exhibit limited stability *in vitro*, even when reconstituted into naturally occurring phospholipid bilayers (Helenius & Simons, 1975; Kuhlbrandt, 1988, 1992).

As an initial step toward characterizing the mechanistic basis of this discrepancy, we decided to test whether synthetic peptides corresponding to the individual α-helices from a polytopic IMP are stable in the TM configuration in isolation from the remainder of the tertiary structure of the protein. We chose to use the prototypical IMP bacteriorhodopsin (BR) for this study because its structure is known at high resolution (Henderson et al., 1990; Grigorieff et al., 1996) and it is one of the few polytopic α-helical IMP's that have been successfully re-folded to the native stable state *in vitro* (Huang et al., 1981; Popot et al., 1987). In this paper, we show that, while four of the seven TM α-helices from BR are stable in the TM configuration on their own, two of them are not. [The seventh helix spontaneously equilibrates between a fully water-soluble stable state, a peripherally membrane-bound state, and a TM α-helical state; the properties of the synthetic peptide corresponding to this helix are described in the accompanying paper by Hunt et al. (1997).] These results represent an exploration of the conformational and thermodynamic constraints on the folding of BR.

EXPERIMENTAL PROCEDURES

Materials. Formic acid (90%) was purchased from J. T. Baker (Phillipsburg, NJ) in polymer characterization solvent grade. 2,2,2-Trifluoroethanol and ethanol were purchased from Lancaster Synthesis (Windham, NH) and Aaper Alcohol and Chemical Company (Shelbyville, KY), respectively.

Buffers. Dilute phosphate buffer (DPB) contained 20 mM NaCl, 5 mM $NaHPO_4$, pH 6.15. SDS buffer contained 5% SDS (w/v), 30 mM $NaHPO_4$, 0.025% NaN_3, pH 8.0. Potassium buffer (KB) contained 150 mM KCl, 30 mM $KHPO_4$, 0.025% NaN_3, pH 6.0.

Peptide Synthesis and Purification. The BR peptides were synthesized using *t*-BOC chemistry by James Elliot at the W. M. Keck Foundation Biotechnology Resource Laboratory at Yale University; they were purified by reversed phase chromatography on a C18 phase using a water/acetonitrile/TFA gradient. The peptides comprise the following residues in the sequence of mature bacteriorhodopsin (see also Figure 1): BR-A = gly-6 through phe-42; BR-B = asp-36 through phe-71; BR-D = val-101 through phe-135; BR-E = thr-128 through glu-166; BR-F = ala-160 through glu-204; and BR-G = ser-193 through ala-233. Both the amino and carboxy termini of all of the peptides are free (*i.e.* unblocked), except for the carboxy terminus of the BR-A peptide which is amidated. A second BR-B peptide was synthesized and characterized containing an identical sequence but an acetylated amino terminus and an amidated carboxy terminus. The biochemical and spectroscopic properties of this second BR-B peptide are very similar to that of the peptide with the free termini with two exceptions: The blocked peptide shows substantially lower solubility in the hydro-organic solvent used for purification of the peptide, and it also shows a lower content of the surface-associated β-sheet structure than the peptide with the free termini when reconstituted into vesicles at an equivalent lipid-to-protein ratio.

Phospholipid Preparation. The polar lipid fraction from *Halobacterium salinarium* (*Halo*-lipids) was isolated using the methods of Kates et al. (1982) as modified by Popot et al. (1987). A stock of *Halo*-lipids containing a trace ^{14}C-label was prepared as described in Hunt et al. (1997) and dissolved in SDS buffer; dissolution was promoted by bath sonication at 45 °C.

Peptide Solubilization. The BR peptides were transferred to SDS buffer by dialysis (Liao et al., 1984; Huang et al., 1981; Popot et al., 1987) after solubilizing them in one of two different organic solvent systems. Peptide samples solubilized in the two different solvent systems were reconstituted and studied independently; for all six BR peptides, identical conformational properties were observed for samples prepared in both ways.

One solvent system comprised a mixture of formic acid, ethanol, and ethanolamine. In this case, the lyophilized peptide was dissolved at 2 mg/mL in 90% formic acid. This solution was diluted with 2 vol of ethanol and then neutralized by the addition of 1 vol of ethanolamine. To dissipate the evolved heat, the ethanolamine was added dropwise while the formic acid solution was held in an ice/water bath. Finally, solid SDS was added at a concentration of 5% (w/v) prior to the initiation of dialysis against SDS buffer. The second solvent system comprised a mixture of water and 2,2,2-trifluoroethanol (TFE). In this case, the lyophilized peptide was dispersed at 2 mg/mL in TFE; this solution was diluted with 1 vol of purified water, and solid SDS was added at a concentration of 5% (w/v) prior to the initiation of dialysis against SDS buffer. Dialysis was performed in Spectrapor 6 dialysis tubing (1000 molecular weight cutoff). The volume of the dialysis buffer was at

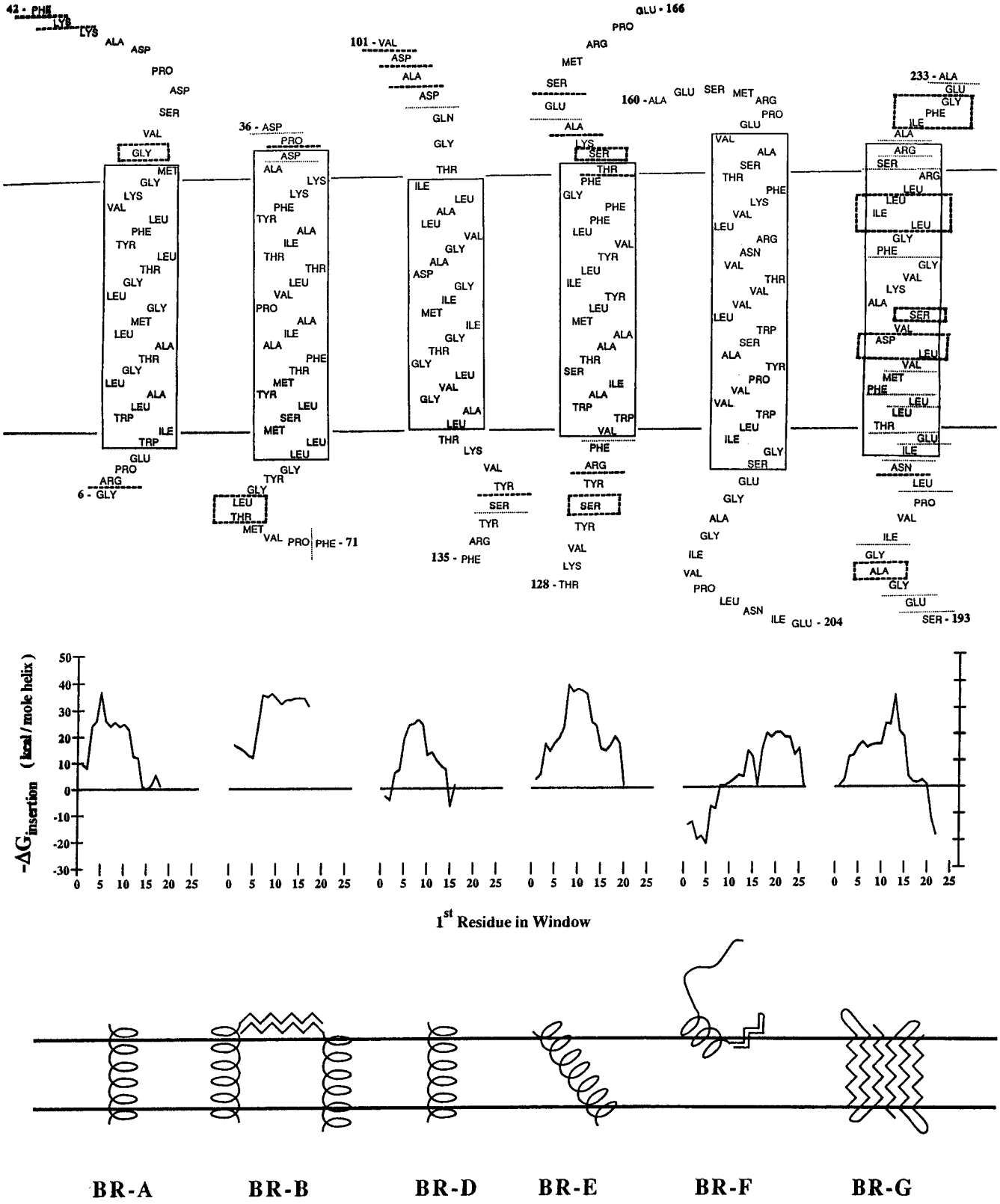

FIGURE 1: Sequences of the synthetic peptides corresponding to the individual transmembrane α-helices in bacteriorhodopsin and schematic summary of their structural properties in reconstituted phospholipid vesicles. The top row in the figure shows the sequences of the six synthetic polypeptides used in these experiments. The solid boxes delineate the experimentally observed limits of the α-helices in the electron crystallographic structure of intact BR (Henderson et al., 1990). The dashed and dotted lines indicate the positions of the protease cleavage sites deduced from the molecular protease protection experiments (see Figure 5), with the lines indicating locations where it was possible to assign the cleavage site to a single peptide bond and the boxes indicating locations where is was only possible to define the cleavage site within a range of peptide bonds. The dashed lines and boxes indicate definitive (*i.e.* unique) assignments, while the dotted lines indicate the locations of all of the possible cleavage sites for the proteolytic fragments for which a unique assignment was not possible. The second row in the figure shows the hydropathy profile of the peptide sequences as calculated using the algorithm of Goldman, Engelman, and Steitz (Engelman et al., 1986). Finally, the bottom row in the figure shows a schematic diagram of the observed conformational properties of the peptides as deduced from the experiments described in this paper.

least 200 times that of the hydro-organic mixture, and the buffer was changed twice during a total period of 48−72 h in dialysis. The buffer had a pH of 8.0 for the initial round of dialysis and a pH of 6.0 for the subsequent two rounds.

Except for the BR-G peptide, which does not contain any tyrosine or tryptophan residues, the concentration of the peptides in the SDS buffer was inferred from the absorbance of the solutions at 280 nm in conjunction with the use of *a priori* extinction coefficients (Cantor & Schimmel, 1980). For the BR-G peptide, the concentration was determined by the use of the bicinchoninic acid assay (Pierce Chemicals, Rockford, IL); this assay was also used to confirm the peptide concentration in many of the other samples. The two concentration estimates agreed within 15% for all of the peptides except BR-D, which appeared to have an anomalously high extinction coefficient.

All of the peptides except the BR-E peptide dissolved immediately in 95% formic acid and also dissolved rapidly and completely in 50% aqueous TFE, suggesting that they are fully soluble in these solvent systems. The solutions containing the BR-E peptide, on the other hand, remained turbid until after the addition of SDS; these solutions cleared slowly over the course of approximately 2 h following the addition of SDS. The BR-E peptide did not seem to be soluble even in neat TFA, once again in contrast to the behavior of the other five BR peptides.

Peptide Reconstitution. The polypeptides were mixed with *Halo*-lipids in SDS buffer at a 5:1 weight ratio of lipid-to-protein, and reconstitution was accomplished using the potassium precipitation technique of Popot et al. (1987) with the addition of 0.5 mM $MgCl_2$ to all of the buffers; in brief, this technique involves collection of the potassium dodecyl sulfate precipitate by low-speed centrifugation followed by extensive dialysis of the vesicles in the supernatant against KB. Following reconstitution, the vesicles were collected by sedimentation in a Ti55 rotor (Beckman Instruments, Palo Alto, CA) at 50 000 rpm and 4 °C for 16 h and then purified by equilibrium density gradient centrifugation on a 5% to 40% (w/v) linear sucrose gradient with a 60% (w/v) sucrose cushion. The gradients contained 200 mM NaCl, 25 mM MES, 0.025% NaN_3, pH 6.15, and were run at 4 °C in either an SW60Ti rotor (17 h) or an SW28 rotor (41 h). The positions of the vesicles were identified visually on the basis of their turbidity, and they were removed from the gradients by piercing the side of the tube with a needle and withdrawing the solution with a syringe. Many of the vesicle preparations exhibited more than one density class on the sucrose gradient, and in these cases, the vesicles in each class were harvested and characterized separately. The reconstituted vesicles were stored in sucrose at −20 °C pending analysis.

Except for the BR-G samples, the peptide concentration in the vesicles was determined by solubilizing a small aliquot in 1% SDS and measuring the absorbance of the resulting solution at 280 nm. The concentration of the BR-G peptide was determined by quantitative amino acid analysis, and this method was used to confirm the peptide concentration in most of the other samples. The phospholipid concentration was determined by scintillation counting using the trace ^{14}C radiolabel. The observed weight ratios of lipid-to-protein in the vesicle preparations were as follows: 4.4:1 for the BR-A peptide; 1.6:1 and 1.9:1 for the BR-B peptide; 1.4:1 2.4:1, 2.6:1, 6.9:1, and 9.7:1 for the BR-D peptide; 4.8:1 and 5.6:1 for the BR-E peptide; 1.0:1, 1.6:1 and 13:1 for the BR-F peptide; and 2.8:1 for the BR-G peptide. Additional samples of the BR-B and BR-F peptides at a lipid-to-protein weight ratio of approximately 5:1 were produced by cosedimentation of protein containing vesicles and pure lipid vesicles. The pellet was frozen and thawed four times prior to resuspension for structural studies. [The molar ratio of phospholipid-to-protein in the vesicles can be calculated based on an average molecular weight of 990 g/mol for the *Halo*-lipids; Kates et al. (1982).] All of the vesicles containing each BR peptide displayed fundamentally equivalent biochemical and spectroscopic properties irrespective of the lipid-to-protein ratio, except for the samples of the BR-D peptide at lipid-to-protein weight ratios lower than or equal to 2.6:1, which showed a mixture of α-helix and β-sheet structure with no well-defined orientation relative to the lipid bilayer (as determined by polarized FTIR spectroscopy).

CD Spectroscopy. Peptide-containing vesicles in sucrose solution were diluted at least 1:1 with pure water and collected by sedimentation for at least 45 min in an A95 rotor in a Beckman Airfuge running at maximum speed. The supernatant was removed using a drawn-out Pasteur pipet, and the pellet was resuspended in DPB/2 (*i.e.* DPB diluted 1:1 with water) by homogenizing it using a Microman M-50 positive-displacement micropipet (Rainin, Woburn, MA). Following resuspension, the vesicles were treated 6 times with a 10 s burst from a microtip probe sonicator at maximum power; CD spectra of these samples were measured at 25 °C within 2 h of the time of sonication (although the spectra were reasonably stable over the course of several days). Peptide samples in SDS buffer were diluted 1:9 with pure water prior to CD measurements. The protein concentration in all of the CD samples was determined by quantitative amino acid analysis and ranged from 40 μg/mL to 120 μg/mL. Spectra were acquired and processed using the same methods described in Hunt et al. (1997) except that samples were measured in a 1.00 mm path length cuvette (Hellma Cells, Jamaica, NY) in the wavelength range from 290 to 185 nm.

The secondary structure content was evaluated using the regularized least-squares algorithm implemented in the program CONTIN (Provencher & Glockner, 1981). For most of the spectra, solutions were chosen with approximately 5 effective degrees of freedom in order to minimize overfitting (Johnson, 1990; Provencher & Glockner, 1981). However, some of the spectra were not fit adequately by such solutions, and, in these cases, solutions were chosen with a higher number of effective degrees of freedom such that the standard deviation of the fit (*i.e.* the discrepancy between the observed and predicted spectra) was roughly consistent for all of the spectra.

Preparation of Macroscopically-Ordered Protein/Phospholipid Multilayers. Vesicles were sedimented out of the sucrose stock solution as described above for the CD measurements and then washed by resuspending them in water and pelleting them a second time using the same protocol. The second pellet was resuspended in approximately 0.7 mL of DPB/150 (*i.e.* DPB diluted 1:149 with water), sonicated as described above, and then filtered through a 0.22 mm polycarbonate syringe filter (CoStar, Cambridge, MA). The filtered samples were stored at −20 °C pending deposition on AgCl windows using isopotential spin-dry centrifugation (Clark et al., 1980) as described in Hunt et al. (1997). The samples contained approximately

225 μg of protein and between 450 μg and 2 mg of phospholipid, depending on the protein sample.

Polarized FTIR Spectroscopy. Polarized FTIR spectra were measured and processed as described in Hunt et al. (1997). The order parameters for the vibrational transition dipole moments that are reported in Table 1 are derived from analysis of complete tilt-series data from each multilamellar film (Rothschild & Clark, 1979a; Earnest et al., 1986). The dichroic ratios of the corresponding absorbances were measured at 4 different angles of incidence (0, 37, 45, and 52° inclination of the surface normal of the sample relative to the incident beam), and the resulting dichroism plots used to perform linear regression analysis are presented in Figure S1 in the Supporting Information. The effective α-helix tilt was calculated based on the observed dichroism of the amide II absorbance using the approach of Rothschild and Clark (1979a) and Earnest et al. (1986); these calculations assumed a value of 1.55 for the refractive index of multilayers, an order parameter of 1.0 for the mosaicity of the multilayers, a mean helix length of 22 residues, and values of 74 and 45.5° for the angle of inclination of the amide II transition dipole moment relative to the axis of an α-helix or β-strand, respectively. The assumed orientation of the amide II transition dipole moment is derived from experimental measurements in the case of the α-helix (Fraser & MacRae, 1973; Nevskaya & Chirgadze, 1976) but from calculations based on ideal secondary structure geometry in the case of the β-strand (Chirgadze & Nevskaya, 1976); an equivalent calculation applied to an idealized α-helix agrees very well with the experimentally measured value of the parameter. The reported range of effective β-strand tilt is derived based on the assumption that the strands comprise 24−40 residues in each monomer of the BR-G peptide.

Amide Exchange Experiments. After recording FTIR spectra from the hydrated film, it was transferred to a dry box (*i.e.* an environment maintained at less than 10% relative humidity using a continuous dry-air purge) where it was dehydrated by storage at room temperature for a minimum of 72 h. After recording FTIR spectra from the dry film in order to confirm dehydration, 8 μL of D_2O was added directly to its surface. The sample was tilted until the liquid had wet the entire surface of the film and then incubated in the dry environment for 15−30 min in order to allow most of the excess D_2O to evaporate. While some bulk D_2O was still visible on the surface of the film, it was transferred to a sealed chamber maintained at a relative humidity of 98% (in D_2O) by a saturated solution of K_2SO_4 in D_2O. After all of the bulk D_2O had evaporated from the surface of the film (approximately 4 h after the addition of the D_2O), the sample was loaded into a compression mount inside the dry box and then mounted in the spectrometer. Polarized FTIR spectra of the sample were measured continuously for the next 15−40 h. The level of deuteration in all samples was monitored by the relative intensity of the O−D *vs* O−H stretching absorbances in the spectra. For all of the D_2O-containing samples presented in this paper, the area ratio of the O−D absorbance to the O−H absorbance was a minimum of 4:1; because the extinction coefficient of the O−D mode is substantially lower than that of the O−H mode, the overall level of deuteration in these samples was very high.

The amide exchange level in the samples was quantitated using simple trapezoid-rule integration of the amide II peaks from the hydrated *vs* deuterated samples; these calculations were performed using the program LabCalc (Galactic Industries, Nashua, NH). The level of exchange in the total population was evaluated based on integration of the peaks in the absolute absorbance spectra collected with perpendicular polarization of the beam relative to the optical plane of incidence, while the level of exchange in the oriented population was evaluated based on integration of the peaks in the dichroism spectra. The spectra to be compared were normalized based on the intensity of the lipid peaks in the absolute absorbance spectra; trapezoid-rule integration was applied to the lipid CH_3 symmetric deformation absorbance centered at 1380 cm^{-1} and/or the lipid CH_2 symmetric stretch absorbance centered at 2830 cm^{-1} (Casal & Mantsch, 1984; Senak et al., 1991) following application of a linear baseline correction locally to each peak. The magnitude of the inferred linear scale factor was typically less than 5% and always less than 15%, and its value was verified on the basis of interactive subtraction of the spectra so as to cancel out the intensity of the lipid absorbances.

Prior to integration of the amide II absorbance, a linear baseline correction was applied to each spectrum using the automated algorithm described in Hunt et al. (1997). The inherent baseline ambiguity in an infrared spectrum gives rise to an uncertainty in the absolute absorbance level which in turn produces a significant uncertainty in quantitating the level of amide exchange, even when a consistent baseline correction is applied to the pre- and post- exchange spectra. Therefore, the level of amide exchange in the samples was evaluated using three different baseline correction protocols in which different pairs of flanking frequencies were adjusted to have zero absorbance: 1780 and 900 cm^{-1}, 1780 and 1300 cm^{-1}, or 1580 and 1490 cm^{-1}. The narrowest interval spanned just the region of the amide II peak itself, and baseline correction in this interval yielded the lowest estimate of protection (*i.e.* the highest estimate of exchange). Table 1 shows the two extreme estimates of protection derived in this way. Note that this ambiguity does not affect quantitation of the exchange level in the dichroism spectra because the baseline is generally consistent between spectra differing only in the polarization of the incident beam.

Protease Protection Experiments. Vesicles were collected out of the sucrose stock solution as described for the CD experiments and resuspended at a protein concentration of 1 mg/mL in a buffer containing 125 mM NaCl, 62.5 mM Tris, pH 8. These solutions were diluted 0.8× in the final reaction mixture. After addition of proteinase K to a working concentration of 50 μg/mL, the samples were subjected to five rounds of freeze−thaw (using liquid nitrogen) immediately prior to incubation at 37 °C for either 2.5 h or 5 h. A concentrated stock solution of the protease at 2.5 mg/mL was stored frozen in 1 mM $CaCl_2$ and diluted further immediately prior to use. CHAPS was used at a final concentration of 2% (w/v) in a subset of the samples. The reactions were stopped by adding phenylmethylsulfonyl fluoride (PMSF) to a final concentration of 2 mM (using a stock solution at 20 mM in isopropyl alcohol); following a 10 min incubation at room temperature, the samples were frozen in liquid nitrogen and lyophilized.

The proteolysis reactions were analyzed using reversed-phase chromatography in a tetrahydrofuran (THF) gradient system. This solvent was chosen because it produces nearly quantitative recovery of large hydrophobic polypeptides

Table 1: Compilation of Summary Data for the Six BR Fragments[a]

	BR-A	BR-B	BR-D	BR-E	BR-F	BR-G	HL
A. CD spectroscopy							
fragments in SDS							
θ_{222} (deg·cm^2/dmol)	16 900	12 800	12 200	17 900	14 200	12 100	
2° structure analysis	68α, 19*β*, 14r	54α, 14*β*, 32r	52α, 25*β*, 23r	76α, 15*β*, 10r	55α, 17*β*, 18r	31α, 44*β*, 24r	
	(5.4, 0.98, 219)	(5.4, 0.98, 242)	(5.4, 0.89, 174)	(5.4, 0.94, 199)	(5.5, 1.00, 155)	(7.6, 0.94, 177)	
fragments in HL							
θ_{222} (deg·cm^2/dmol)	22 100	15 700	17 500	18 000	13 700	13 200	
2° structure analysis	74α, 26*β*	58α, 5*β*, 37r	78α, 7*β*, 14r	80α, 7*β*, 13r	50α, 37*β*, 13r	17α, 63*β*, 20r	
	(7.2, 1.03, 253)	(5.4, 0.98, 185)	(5.2, 0.87, 228)	(5.5, 0.91, 230)	(9.5, 1.04, 453)	(7.5, 0.92, 317)	
B. FTIR spectroscopy							
⊥ absorbance							
amide I band (cm^{-1})	1658	1654 (1637)	1655 (1632)	1655	1649	1628 (1654,1691)	[1652][c]
amide II band (cm^{-1})	1550	1545	1547	1547	1547	1541	
phosphate band (cm^{-1})	1219	1224	1215	1219	1217	1216	1219
lipid bands (cm^{-1})	1462, 1378	1462, 1378	1463, 1378	1464, 1379	1464, 1378	1463, 1379	1463, 1378
dichroism							
amide I band (cm^{-1})	1660	1662	1655	1656	1684	1624 (1696)	
amide II band (cm^{-1})	1551	1545	1547	1547		1535	
$\langle P_2\rangle_{A_{II}}$, ⟨helix tilt⟩	−0.25, 0°	−0.14, 32°	−0.15, 31°	−0.06, 44°		+0.15, 0°− 31° [b]	
phosphate band (cm^{-1})	1217	1215	1214	1214	1212	1211	1217
$\langle P_2\rangle_{PO_4}$	−0.16		−0.16	−0.09	−0.17	−0.08	−0.12
lipid C−O−C band (cm^{-1})	1146	1155	1145	1143	1148	1147	1140
$\langle P_2\rangle_{C-O-C}$	+0.16		+0.16	+0.11	+0.15	+0.07	+0.10
C. amide exchange							
protected at 4−6 h							
all protons (%, no.)	67%, 25	65%, 23	74%, 26	57%, 22	25%, 11	62%, 25	
	(51%, 19)	(60%, 21)	(58%, 20)	(48%, 18)	(16%, 7)	(39%, 16)	
oriented protons (%)	93%	72%	88%	89%		93%	
exchange time (h)	5.4	4.5	4.4	4.2	4.6	4.5	
protected at 16−37 h							
all protons (%, no.)	64%, 24	66%, 24	51%, 18	60%, 23	22%, 10	64%, 26	
	(51%, 19)	(62%, 22)	(51%, 18)	(46%, 18)	(16%, 7)	(42%, 17)	
oriented protons (%)	94%	70%	76%	77%		91%	
exchange time (h)	36.8	20.6	18.6	16.0	15.9	16.7	
D. protease protection							
pristine mass (H^+ ion)	4039.8	4001.8	3587.2	4675.5	4900.7	4319.2	
control vesicles							
m/*z*, assignment	4039, (1−37)	4000, (1−36)	2934, (2−31)	4674, (1−39)	4899, (1−45)	4320, (1−41)	
	4055, (1−37)·O	4018, (1−36)·O	*3186, (2−32)*	4690, (1−39)·O	4916, (1−45)·O	4337, (1−41)·O	
	4070, (1−37)·O_2	4031, (1−36)·f	*(5−35)*	4704, (1−39)·f	4928, (1−45)·f	4348, (1−41)·f	
	4087, (1−37)·O_3	4041, (1−36)·K	3300, (4−35)	4718, (1−39)·O·f	4940, (1−45)·K	4359, (1−41)·K	
		4055, (1−36)·f_2	3316, (4−35)·O	4732, (1−39)·f_2	4954, (1−45)·f_2	4374, (1−41)·O·K	
		4072, (1−36)·O·f_2	3375, (3−35)	4747, (1−39)·f_2·O	4970, (1−45)·O·f_2		
		4086, (1−36)·O·f·K	3389, (3−35)·O		4983, (1−45)·f_3		
		4093, (1−36)·f_2·K	3586, (1−35)				
			3603, (1−35)·O				
			3622, (1−35)·O_2				

Table 1: (Continued)

	BR-A	BR-B	BR-D	BR-E	BR-F	BR-G	
D. protease protection (contd.) vesicles + proteinase K							
m/*z*, assignment	*2997, (1−27)*	*3314, (1−30)*	*3318, (4−35)·O*	2816, (7−29)		*1931, (2−19)*	*3108, (9−36)·O*
	(2−28)	*(2−31)*	3318, (4−35)·O	*2916, (7−30)*		*(3−20)·O*	*(10−37)·O*
	3010, (1−27)·O	*(3−32)*	3372, (3−35)*	*(9−33)*		*(19−36)·O*	3496, (10−41)
	(2−28)·O	*3527, (1−32)**	3388, (3−35)·O	*2932, (7−30)·O*		*(20−37)·O*	3512, (10−41)·O
	3025, (1−27)·O_2	*(4−35)**	3588, (1−35)	*(9−33)·O*		*1975, (5−22)*	*3716, (2−36)*
	(2−28)·O_2	*3542, (1−32)·O*	3603, (1−35)·O	*3167, (5−30)*		*(4−21)·O*	*(5−38)*
	3765, (1−35)*	*(4−35)·O*		*(6−31)*		*1980, (16−33)*	*(6−39)*
	3781, (1−35)·O	*3555, (1−32)·f*		3873, (1−32)*		*(9−26)·O*	*3732, (2−36)·O*
	3796, (1−35)·O_2	*(4−35)·f*		3902, (1−32)·f		*2069, (16−34)*	*(5−38)·O*
	3804, (1−35)·K	*3562, (1−32)·O_2*		3930, (1−32)·f_2		*(10−28)·O*	*(6−39)·O*
	3821, (1−35)·O·K	*(4−35)·O_2*		4073, (1−34)		*(11−29)·O*	*3975, (2−38)**
	3804, (1−35)·K	*3581, (1−32)·f_2*		4102, (1−34)·f		*(12−30)·O*	*(4−40)**
	3821, (1−35)·O·K	*(4−35)·f_2*		4674, (1−39)		*2185, (9−28)·O*	*(5−41)**
	3836, (2−36)*	*3596, (1−32)·O·f_2*		4690, (1−39)·O		*(10−29)·O*	*3992, (2−38)·O*
	3851, (2−36)·O	*(4−35)·O·f_2*		4704, (1−39)·f		*(11−30)·O*	*(4−40)·O*
	4039, (1−37)	3806, (3−36)·O		4718, (1−39)·O·f		*(12−31)·O*	*(5−41)·O*
	4055, (1−37)·O	4001, (1−36)				*2551, (11−33)*	*4014, (2−38)·K*
	4070, (1−37)·O_2	4017, (1−36)·O				*(13−35)*	*(4−40)·K*
		4033, (1−36)·O_2				*(5−28)·O*	*(5−41)·K*
		4047, (1−36)·O·f				*(18−41)·O*	*4030, (2−38)·O·K*
		4055, (1−36)·f_2				*2906, (2−29)*	*(4−40)·O·K*
						(10−35)	*(5−41)·O·K*
						2922, (15−41)	4320, (1−41)
						(2−29)·O	4336, (1−41)·O
						(10−35)·O	4359, (1−41)·K
						2993, (9−36)	4374, (1−41)·O·K
						(10−37)	

[a] A. The secondary structure content in the CD spectra of the fragments as estimated using the program CONTIN. Secondary structure is assigned to either α-helix (α), *β*-sheet (*β*), or remainder (r); the three values in parentheses represent the number of degrees of freedom in the fit, the normalized protein concentration, and the standard deviation of the fit, respectively. B. The peak frequencies (with shoulder frequencies in parentheses) from the FTIR spectra of the macroscopically oriented protein/phospholipid multilayers as well as the inferred order parameters for the indicated vibrational transition dipole moments and the corresponding α-helix tilt or [b] *β*-strand tilt for the BR-G peptide. The tilt angles are estimated based on an α-helix comprising 22 residues or a *β*-sheet comprising 24−40 residues. [c] The number in square brackets is the frequency of the underlying H_2O scissoring absorbance. C. The proportion of protected amide bonds in the total population as quantitated based on the absolute absorbance spectra, and the proportion of protected amide bonds in the oriented population as quantitated based on the dichroism spectra. Two limiting estimates of the exchange level are given for the total amide bond population derived from different baseline assignment protocols. D. The *m*/*z* values for the observed ion peaks are indicated along with the inferred sequence assignment for the molecular species; formylated ions, oxygenated ions, and potassium adducts are indicated by •f, •O, and •K, respectively. The *m*/*z* values and the sequences of all of the various candidate peptides are printed in italics when it was not possible to uniquely assign a species to a single proteolytic product. The dominant proteolysis products in the presence of proteinase K are indicated by asterisks.

(Hunt, 1993). A 4.6 mm internal diameter × 75 mm micropellicular (Kalghatgi & Horváth, 1987) HyTach C18 column (Glycotech, Hamden, CT) was run at 50 °C using a flow rate of 1.0 mL/min. The samples were loaded onto the column in 0.5 mL of 90% formic acid. The gradient profile was as follows: 8 min isocratic at 28.5% THF; 10 min linear gradient to 95% THF; 2 min isocratic at 95% THF. All eluents contained 0.1% trifluoroactetic acid (TFA). Column fractions were collected at 1 min intervals; they were lyophilized immediately at the end of each column run and stored at −20 °C pending further analysis.

Mass Spectrometry. Mass spectrometry was performed by W. J. McMurray and G. Giordano at the Biochemical Mass Spectrometry Facility at the Yale University School of Medicine. The lyophilized column fractions were dissolved in concentrated TFA and spotted onto a matrix of *m*-nitrobenzyl alcohol prior to analysis using a double-focusing mass spectrometer (VG Analytical, Manchester, U.K.) equipped with a cesium ion fast atom bombardment (FAB) probe (Senko & McLafferty, 1994). All of the column fractions showing significant absorbance at 215 nm were scanned in a mass range starting at *m*/*z* 2000 and extending up to a value of *m*/*z* at least 500 greater than the atomic weight of the pristine polypeptide; usually, two independent scans were required to cover the entire mass range. Most of the column fractions were also scanned in the mass range from *m*/*z* 800 to *m*/*z* 2000. For each spectrum, the data from an appropriate series of scans were averaged and deconvolved using standard techniques.

The deconvolved mass spectra of the column fractions from vesicles incubated in the absence of protease showed primarily a single cluster of ion peaks starting at the molecular weight of the pristine peptide (with at most a minor content of readily assignable peptide fragments presumably derived from proteolysis during storage) plus a series of lipid-derived peaks in the *m*/*z* range from 900 to 1500 in the later column fractions. In addition to the protonated peptide ion, mass species were frequently observed at +16, +28, and +38 atomic mass units (plus linear combinations of these increments); these species were interpreted as the mono-oxygenated peptide, the monoformylated peptide, and the potassium salt of the peptide, respectively. We believe that methionine side chains represent the most likely sites for oxidation. The mass spectra of the proteolyzed samples were analyzed by comparing the masses of the observed ions against a matrix filled with the masses of all possible peptide subfragments. The masses of the potassium salts of all of the subfragments were also considered, as were the masses of the various covalent derivatives of the subfragments when the corresponding derivatives were observed in the mass spectrum of the unproteolyzed peptide. The discrepancies between observed and calculated *m*/*z* values were usually within ±2 and always within ±3.

RESULTS

Peptide Design and Reconstitution into Vesicles. Polypeptides corresponding to each of the seven transmembrane α-helices in the native tertiary structure of BR were chemically synthesized. We designed each polypeptide to include the entire transmembrane helix (Grigorieff et al., 1996) plus some portion of the flanking sequences (Figure 1). On the basis of our initial experiences with polypeptides corresponding to the A and B helices of BR, we concluded that the charge density at the termini of the hydrophobic transmembrane sequences is a critical factor in determining the overall solubility properties of the polypeptides. Because solubilization in hydro-organic mixtures is required for both purification and reconstitution, this observation placed a significant constraint on our design strategy. Except for the BR-B helix, most of the residues in the interhelix loops on both sides of a given helix are included in the synthetic polypeptide in order to satisfy this constraint. The lengths of the flanking sequences included in the polypeptides range in size from two residues at the amino terminus of the polypeptide corresponding to the B helix to eleven residues at the carboxy terminus of the polypeptide corresponding to the F helix (see Figure 1 for details).

All seven polypeptides were designed and synthesized prior to the availability of the high-resolution electron density map of bacteriorhodopsin, *i.e.* when the map was good enough to identify the presence of seven transmembrane helices (Baldwin et al., 1988) but not good enough to assign the primary sequence of the protein to the observed structural features (Henderson et al., 1990). Thus, our assignment was based on the use of the hydropathy algorithm of Goldman, Engelman, and Steitz (Engelman et al., 1986). In Figure 1, the extent of the α-helices eventually deduced from the electron density map of Henderson et al. (1990) is indicated by the rectangular boxes superimposed on the polypeptide sequences. We were successful in identifying the approximate locations of all seven α-helices using the hydropathy algorithm alone.

In preparation for structural studies, the synthetic polypeptides were dissolved in the detergent sodium dodecyl sulfate (SDS) and then reconstituted into phospholipid vesicles using a polar lipid extract from *H. salinarium* (Kates et al., 1982). Reconstitution was accomplished by potassium precipitation of the dodecyl sulfate, followed by extensive dialysis (Popot et al., 1987); this procedure has previously been used to regenerate the native structure of BR following denaturation of the protein in SDS (Popot et al., 1986). The reconstituted vesicles were purified by sucrose density gradient centrifugation prior to characterization. We found that six of the seven polypeptides are stably and irreversibly associated with the phospholipid vesicles following reconstitution near neutral pH; the structural characterization of these polypeptides is reported in this paper. The seventh polypeptide, that corresponding to the BR-C helix, spontaneously equilibrates between a soluble form and a membrane-associated form in a pH-dependent fashion; the structural properties of this polypeptide are described in the accompanying paper.

CD Spectroscopy of Vesicles in Solution. Figure 2 shows normalized circular dichroism (CD) spectra of the BR-A, BR-B, BR-F, and BR-G peptides either dissolved in SDS buffer or reconstituted into *Halo*-lipid vesicles. (The CD spectra of the BR-D and BR-E peptides are shown in Figure S1 in the Supporting Information for this paper.) The samples in SDS buffer represent the material used for reconstitution. Quantitative analysis of the secondary structure content in the CD spectra of all six peptides was performed using the program CONTIN (Provencher & Glockner, 1981) and is summarized in Table 1. Except for BR-G, all of the peptides show predominantly α-helical secondary structure in both environments (Johnson et al., 1988; Johnson, 1990). The spectra of the BR-A, BR-B, BR-D, and BR-E peptides in *Halo*-lipid vesicles exhibit all of the qualitative spectral characteristics expected for a strongly

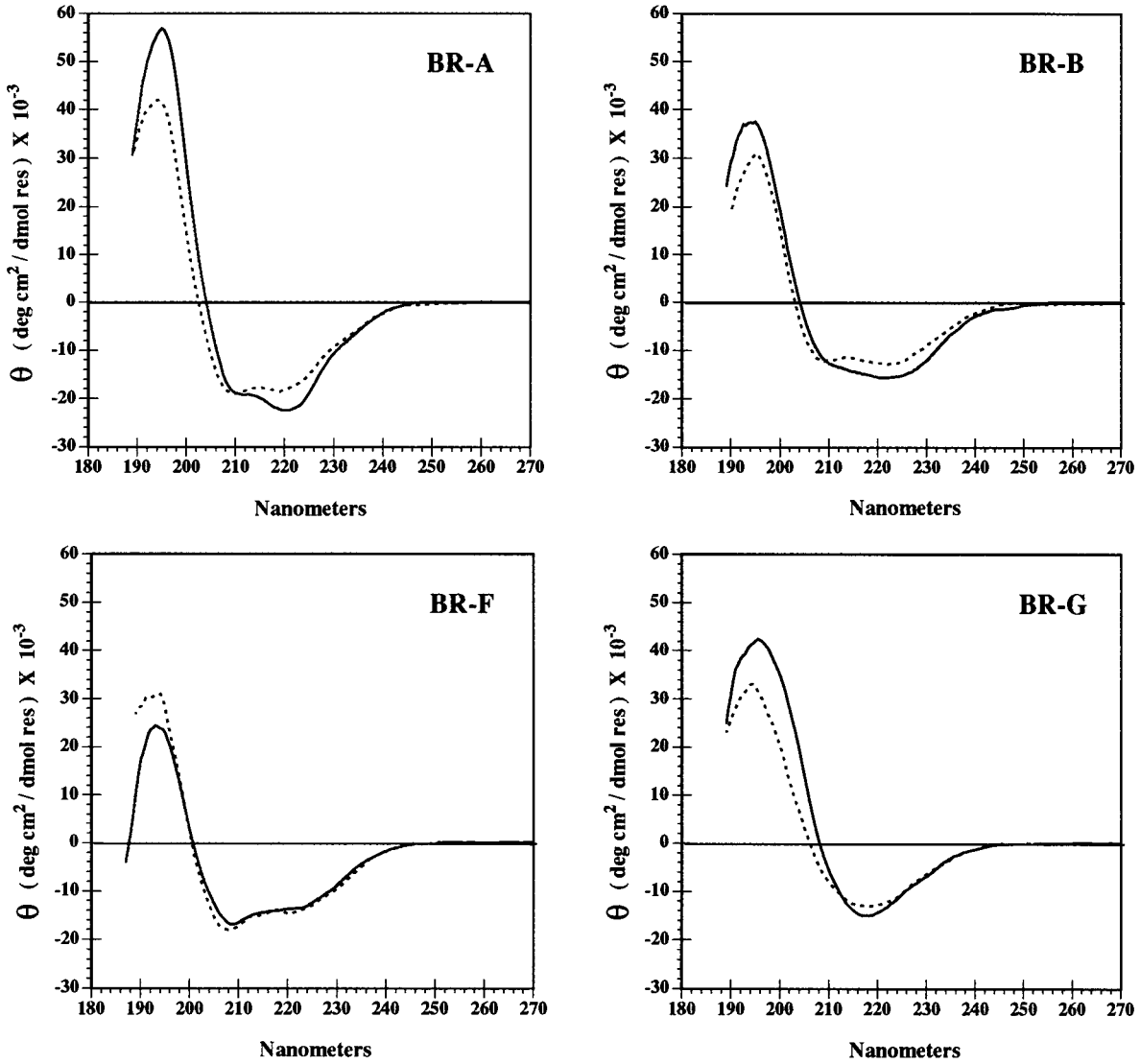

FIGURE 2: CD spectroscopy of the individual BR helices in SDS and in phospholipid bilayers. The dotted lines represent the data for the peptides in SDS, while the solid lines represent the data for the peptides in *Halo*-lipid vesicles. Pure *Halo*-lipid vesicles produce a negligible CD signal at the concentrations used in these experiments (data not shown). The CD spectra of the BR-D and BR-E peptides are shown in Figure S1 in the Supporting Information for this paper.

α-helical sample: double minima at 222 and 208 nm and a ratio of the magnitude of the molar ellipticity at 195 *vs* 222 nm greater than or equal to 2.5:1 (Johnson, 1988). Furthermore, the magnitude of the mean residue ellipticity at 222 nm observed in these spectra as well as curve fitting analysis are consistent with the presence of an α-helix of at least 20 residues in length in each of the four polypeptides. For reference, the CD spectrum of the BR-A peptide is very similar in both its shape and its normalized magnitude to that of intact BR reconstituted into small unilamellar phospholipid vesicles (Mao & Wallace, 1984).

Quantitative analysis of the spectrum of the BR-F peptide in *Halo*-lipid vesicles indicates a lower α-helix content (*i.e.* 50% *vs* 58%−80%) and a significantly higher β-sheet content (*i.e.* 37% *vs* 5%−26%) compared to the BR-A, BR-B, BR-D, and BR-E peptides. The qualitative features of the BR-F spectrum also suggest a lower α-helix content, especially the weak maximum at 195 nm (∼24 000 deg cm²/decimol) and the low ratio of the magnitude of the molar ellipticity at 195 *vs* 222 nm of less than 2:1. The BR-F peptide is also the only one (other than BR-G) to show a lower α-helix content in *Halo*-lipid vesicles than in SDS.

The BR-G peptide shows predominantly β-sheet secondary structure both in SDS and in *Halo*-lipid vesicles (Figure 2 and Table 1), with its CD spectrum displaying a single minimum at 218 nm (Johnson, 1988). The persistence of the β-structure in SDS buffer is remarkable because SDS generally induces α-helical conformation in proteins and peptides. To test the thermodynamic stability of this structure, we heated both samples of the BR-G peptide to 100 °C for 5 min and then re-collected their CD spectra after allowing the samples to re-equilibrate at 25 °C. The spectra were essentially identical before and after heating (data not shown), indicating that the β-sheet structure either is stable at high temperature or re-forms spontaneously upon cooling. A sample of the BR-G peptide in *Halo*-lipid vesicles was also titrated to extremes of acidic and basic pH (pH < 4 and pH > 9); the spectra acquired under these conditions were essentially identical to those acquired near neutral pH (data not shown).

Polarized FTIR Spectroscopy of Macroscopically-Ordered Protein/Phospholipid Multilayers. Figure 3 shows polarized Fourier transform infrared (FTIR) spectra of macroscopically oriented protein/phospholipid multilayers made from vesicles containing the BR-A, BR-B, BR-E, BR-F, and BR-G peptides as well as from pure *Halo*-lipid vesicles. Summary data derived from equivalent experiments on all six BR peptides are collected in Table 1. (The corresponding

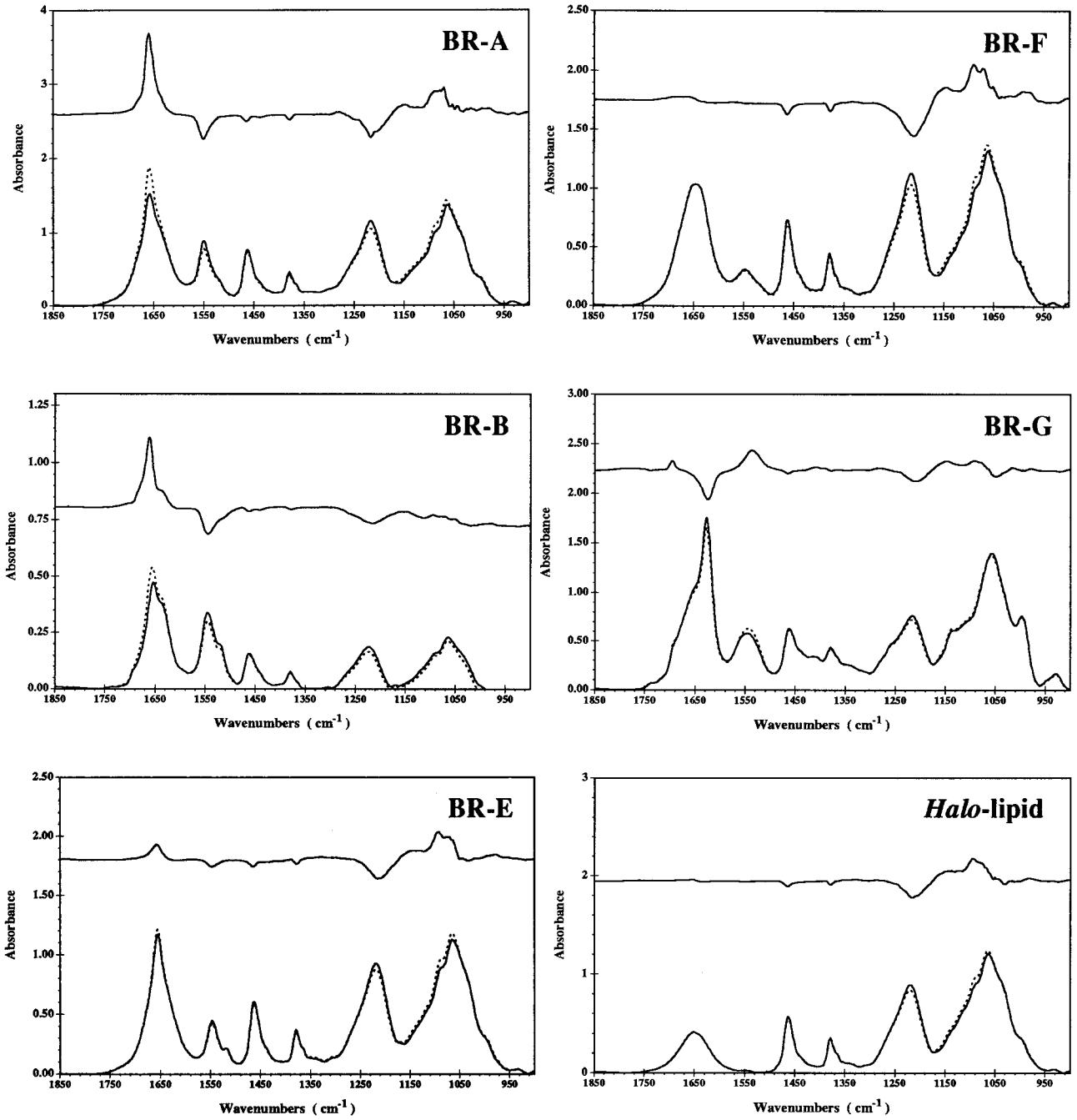

FIGURE 3: Polarized FTIR spectroscopy of the individual BR helices in macroscopically ordered phospholipid multilayers. The lower traces in each panel represent the absolute absorbance spectra of the sample acquired with the incident beam polarized either parallel (dotted line) or perpendicular (solid line) to the optical plane of incidence (Earnest et al., 1986). The upper trace represents the difference between the spectra acquired with the two polarizations of the incident beam multiplied by a factor of 3. All of the spectra were acquired at an angle of incidence of 45° (relative to the plane of the sample substrate). The polarized FTIR spectrum of an equivalent sample containing the BR-D peptide is shown in Figure S2 in the Supporting Information, which also presents dichroism plots (in Figure S3) quantitating the variation in the dichroic ratio as a function of the angle of incidence for a set of protein and lipid absorbances in each of the multilamellar samples examined here.

spectrum from a sample of the BR-D peptide is shown in Figure S2 in the Supporting Information, while dichroism plots, which quantitate the variation in the observed dichroic ratio of a set of protein and lipid absorbances as a function of the sample tilt angle, are presented for all of the multilamellar samples in Figure S3 in the Supporting Information.)

Polarized FTIR allows characterization of the orientation of the protein secondary structure relative to the plane of the phospholipid bilayer (Rothschild & Clark, 1979a; Nabedryk et al., 1988; Kleffel et al., 1985). Specifically, when phospholipid vesicles are equilibrated at high relative humidity in the absence of bulk water, a multilamellar phase is formed in which the plane of the individual constituent bilayers is oriented parallel to the macroscopic sample plane (Zaccaï et al., 1979; Büldt et al., 1979; Popot et al., 1986). In general, the introduction of proteins or peptides into the bilayers does not affect either the structure or orientation of the multilamellar phase (Nabedryk et al., 1988; Nabedryk & Breton, 1981; Engelman et al., 1986). In particular, control experiments have been performed in which intact BR was reconstituted into *Halo*-lipid vesicles which were then deposited as protein/phospholipid multilayers (Earnest, 1987; Hunt, 1993). These experiments establish that protein-containing bilayers still form well-ordered multilayers, and they have also been used to calibrate the magnitude of the

spectroscopic signal expected for well-oriented and stable transmembrane α-helices (Rothschild & Clark, 1979a; Earnest et al., 1986, 1990; Earnest, 1987).

The BR-A, BR-B, BR-D, and BR-E peptides all show evidence of α-helical secondary structure oriented perpendicular to the plane of the membrane, displaying positive dichroism in the protein amide I absorbance at approximately 1657 cm^{-1} (primarily a carbonyl stretching mode) and negative dichroism in the protein amide II absorbance at approximately 1546 cm^{-1} (a coupled N−H rocking and C−N stretching mode). Because of the absence of overlapping spectral features, the amide II absorbance provides the most reliable quantitation of the protein backbone orientation (Rothschild & Clark, 1979a; Earnest et al., 1986). The magnitude of the amide II dichroism for the BR-A peptide is identical to that observed for intact BR, indicating that essentially all of the peptide molecules must form α-helices with a transbilayer orientation.

Although the spectra of the BR-B, BR-D, and BR-E peptides display the same qualitative features as the spectrum of the BR-A peptide, the magnitude of the amide II dichroism is lower in these samples (Table 1). The observed dichroism is consistent with all of the peptide molecules forming stable transmembrane α-helices tilted away from the membrane normal by either approximately 30° for the BR-B and BR-D peptides or approximately 45° for the BR-E peptide. From the FTIR spectra alone, we cannot exclude the possibility that the samples comprise a mixture of populations with different conformational properties, *e.g.* one population comprising untilted transbilayer α-helices plus another population comprising either α-helices lying flat on the surface of the membrane or disordered structures without any net peptide bond orientation. However, even if there are multiple conformational populations, a significant fraction of the peptide molecules must have a transmembrane orientation in these samples. Furthermore, at least for the BR-E peptide, protease protection experiments suggest that all of the individual peptide molecules have the same conformational properties (see below), indicating that there is either a homogeneous population or a dynamic equilibrium between the various populations. In contrast to all of the other α-helices in the native structure of BR, there are clusters of aromatic residues at both tips of the BR-E helix; for both of these distal regions to interact simultaneously with the hydrophobic core of the bilayer, the axis of the α-helix would have to tilt down toward the plane of the bilayer (Brasseur, 1991). The apparent level of the lipid dichroism in the BR-E sample is lower than that in most of the other peptide-containing multilayers (see below), and perturbation of the lipid orientation could potentially weaken the protein dichroism of an untilted α-helix. However, the quantitative reliability of the lipid dichroism is limited because of its very weak magnitude, so that we believe that the larger tilt angle inferred for the BR-E helix probably reflects a real difference in the net orientation of this helix in the phospholipid membranes.

The dichroism spectrum of the BR-B peptide (Figure 3) shows fine structure in its amide I absorbance profile in addition to the strong α-helical peak at 1662 cm^{-1}. The presence of the positive shoulder at 1635 cm^{-1} and the very weak negative feature at 1695 cm^{-1} are consistent with the presence of a small amount of antiparallel β-sheet in this sample (Krimm & Bandekar, 1986; Chirgadze & Nevskaya, 1976; Nabedryk et al., 1988; Kleffel et al., 1985; Earnest et al., 1990). On the basis of the sign of the dichroism, the strands of this sheet are oriented parallel to the plane of the membrane while the carbonyl bonds are oriented perpendicular to the plane of the membrane (Fraser & MacRae, 1973; Suzuki, 1967; Nabedryk et al., 1988; Kleffel et al., 1985; Challou et al., 1994). Given this orientation, it is very likely that the β-sheet structure is associated with the surface of the membrane rather than the hydrophobic core. In a series of BR-B samples with varying lipid-to-protein ratios, the magnitude of the β-sheet signal in the dichroism spectrum increases in proportion to the concentration of the peptide in the bilayer (data not shown), suggesting that the β-sheet may be formed by inter-peptide interactions. In samples at a constant lipid-to-protein ratio, a higher content of this structure is observed when the amino and carboxy termini of the peptide are unblocked compared to when they are acetylated and amidated, respectively (see Experimental Procedures). This observation suggests that the β-structure includes a sequence near at least one terminus of the BR-B peptide, and we speculate that it is likely to involve the C-terminal octapeptide on the basis of the high β-propensity for this sequence in Chou−Fasman analysis (Fasman & Chou, 1978). This region of the BR-B peptide forms part of the largest interhelical loop in the native structure of BR.

The dichroism spectrum of the BR-F peptide does not show any evidence of oriented protein secondary structure of any kind. The broad envelope of the amide I peak in the absolute absorbance spectra of this peptide indicates a mixture of α-helical structure absorbing at approximately 1655 cm^{-1} plus a substantial fraction of β-sheet structure absorbing at approximately 1635 cm^{-1}. This observation is consistent with the results from CD spectroscopy showing a qualitatively lower α-helix content and higher β-sheet content in the vesicles containing this peptide compared to the vesicles containing the BR-A, BR-B, BR-D, and BR-E peptides. We conclude that there is little tendency for the synthetic peptide corresponding to the F helix to adopt a transbilayer α-helical conformation in the *Halo*-lipid multilayers under the same conditions that produce transbilayer α-helices in the others. The spectra shown in Figure 3 were obtained from samples containing approximately a 13:1 weight ratio of lipid-to-protein; samples containing a 1:1 weight ratio of lipid-to-protein showed essentially identical spectroscopic and biochemical properties (data not shown).

In contrast, the dichroism spectrum of the BR-G peptide shows evidence of a strongly oriented β-sheet structure (Figure 3). The intense amide I peak at 1628 cm^{-1} in the absolute absorbance spectra of this peptide indicates that it contains predominantly β-type secondary structure; the associated shoulder at 1690 cm^{-1} suggests that the β-sheet has an antiparallel structure (Krimm & Bandekar, 1986; Chirgadze & Nevskaya, 1976; Nabedryk et al., 1988; Kleffel et al., 1985). Once again, the results of FTIR spectroscopy of multilayers are consistent with the conclusions drawn from CD spectroscopy of vesicles in solution. The negative peak at 1624 cm^{-1} in the amide I region of the dichroism spectrum indicates that the carbonyl bonds in the β-sheet are directed more or less parallel to the plane of the bilayer, while the positive peak at 1541 cm^{-1} in the amide II region indicates that the polypeptide backbone is oriented more or less perpendicular to the plane of the membrane (Fraser & MacRae, 1973; Suzuki, 1967; Kleffel et al., 1985; Nabedryk et al., 1988). Quantitative analysis of the amide II dichroism indicates that the β-strands of the peptide can be tilted at

most 31° from the normal to the plane of the membrane even if every residue is incorporated in the β-sheet (Table 1). Such an orientation is consistent with the formation of a transmembrane β-sheet structure. In any event, the intense dichroism of the amide absorbances requires that the strands of the β-sheet must either penetrate into the core of the membranes or extend upward from the surface of the membranes in the multilamellar sample.

The dichroism of the phospholipid absorbances is very similar in the FTIR spectra of all of the protein-containing multilayers as well as in the pure *Halo*-lipid multilayers (Table 1 and Figure S3). X-ray diffraction experiments have established that this phospholipid preparation forms a well-behaved multi-bilayer phase at high relative humidity (Popot et al., 1986). The dichroism of the phospholipid absorbances provides a direct measure of the structure of the phospholipid phase in our FTIR samples. The opposite sign of the dichroism in the phosphate antisymmetric stretching absorbance at approximately 1215 cm^{-1} compared to the adjacent ether stretching absorbance at approximately 1145 cm^{-1} provides a stringent control on the orientation of the phospholipid molecules (as well as on the validity of the dichroism data). Given the large amount of phospholipid in some of the films, the optical absorbance in the CH-stretching region is greater than 2.5 in most of the samples, so that the phosphate absorbance is also the most highly dichroic and the most intense phospholipid feature that can be quantitated accurately. Compared to the pure *Halo*-lipid multilayers, the magnitude of the lipid dichroism seems to be slightly higher in the films containing the BR-A, BR-D, and BR-F peptides and slightly lower in the films containing the BR-E and BR-G peptides (Table 1 and Figures 3, S2, and S3). These differences may derive from inaccuracy in quantitating a small signal, or they may reflect minor perturbations in the average orientation of the phospholipid molecules in the vicinity of the reconstituted polypeptides (Jordi et al., 1990; Van Zoelen et al., 1978; Batenburg et al., 1987). However, it is very likely that a multi-bilayer phase is maintained in all of the samples. The spectra of the BR-B peptide shown in Figure 3 were collected from a sample that contained a low 1.4:1 lipid-to-protein weight ratio. Although the BR-B helix remains well-oriented relative to the phospholipid bilayers in this sample, the concentration of phospholipid is too low to allow reliable quantitation of its weak dichroism signal; the conformational properties of this peptide were equivalent in samples at higher lipid-to-protein weight ratios in which the dichroism of the phospholipid vibrations was observed to be similar to that in the samples of the other peptides (data not shown).

The α-helical BR peptides all display relatively normal amide I vibrational frequencies near 1656 cm^{-1} compared to the anomalously high amide I frequency of intact BR in purple membrane at ~1662 cm^{-1} (Rothschild & Clark, 1979b). This observation suggests that the anomalous vibrational properties of purple membrane could derive from helix−helix interactions and potentially from transition dipole moment coupling (Krimm & Abe, 1972; Nevskaya & Chirgadze, 1976) between the oscillators in different α-helices in a tightly-packed parallel/antiparallel array (Hunt, 1993).

Amide Exchange Experiments in Protein/Phospholipid Multilayers. The results of amide exchange experiments conducted on the multilamellar films containing the BR-A, BR-B, BR-F, and BR-G peptides are presented in Figure 4, and data derived from equivalent experiments on all six BR peptides are summarized in Table 1. (The corresponding FTIR spectra for samples of the BR-D and BR-E peptides are shown in Figure S4 in the Supporting Information for this paper.) Amide exchange (*i.e.* H/D or $^1H/^2H$ exchange) experiments are used in structural studies of proteins to characterize the dynamics of the polypeptide backbone (Sami & Dempsey, 1988; Osborne & Nabedryk-Viala, 1978; Rath et al., 1991; Miranker et al., 1991; Prestrelski & Arakawa, 1991; Earnest et al., 1990; Zhang et al., 1992). It is believed that the rate of exchange of the individual amide protons on the polypeptide backbone is determined primarily by the stability of the protein secondary structure involving those residues (Roder, 1989; Englander & Mayne, 1992; Dempsey et al., 1991; Miranker et al., 1996). Moreover, in the case of transmembrane secondary structure, it can be assumed that the polypeptide backbone cannot undergo amide exchange if it is localized in the hydrocarbon core of the phospholipid bilayer since this would require disruption of the backbone hydrogen bonding pattern and exposure of the highly polar peptide bonds in an extremely hydrophobic environment (Zhang et al., 1992; Earnest et al., 1990; Holloway & Buchheit, 1990). In FTIR spectroscopy, backbone H/D exchange produces a major shift in the frequency of the amide II absorbance from approximately 1540 cm^{-1} to approximately 1440 cm^{-1} but only a minor decrease in the frequency of the amide I absorbance on the order of 1 cm^{-1}.

Polarized FTIR spectra of the multilamellar films were monitored continuously starting 4−5 h after the initiation of the H/D exchange reaction and continuing for at least an additional 12 h. The spectra shown in Figure 4 were acquired from samples after a minimum of 16 h of continuous exposure to D_2O, except for the spectra of the sample containing the BR-F peptide, which were acquired after only 4 h of continuous exposure to D_2O. With the possible exception of the BR-D sample, the overall level of D_2O exchange observed after 4−6 h of exposure is equivalent to that observed after 16−37 h of exposure (Table 1). For all of the peptides except BR-F, between 42% and 66% of the amide protons are protected from H/D exchange at the later time point, corresponding to an average of at least 17 protected residues in each peptide molecule. The protected residues must be participating in some kind of structural interaction which prevents their backbone protons from exchanging with bulk solvent; the most likely explanation is that they are sequestered in stable protein secondary structure. In contrast, at most 25% of the amide protons on the BR-F peptide are protected from H/D exchange after 3 h, corresponding to an average of at most 11 protected residues in each peptide molecule. This observation suggests that the extent of stable secondary structure in the BR-F peptide in association with the phospholipid vesicles is low. The difference in the amide exchange behavior of the BR-F peptide compared to the other five BR peptides reinforces the conclusion that this peptide does not adopt a stable transbilayer α-helical conformation in phospholipid membranes.

Although the absolute absorbance spectra of the multilamellar films indicate that all of the peptides experience a significant level of H/D exchange of their backbone protons, the dichroism spectra uniformly show a lower level of exchange. At least 70% of the oriented backbone protons are protected in the BR-B peptide and even higher levels are protected in the other peptides (Figures 4 and S4 and

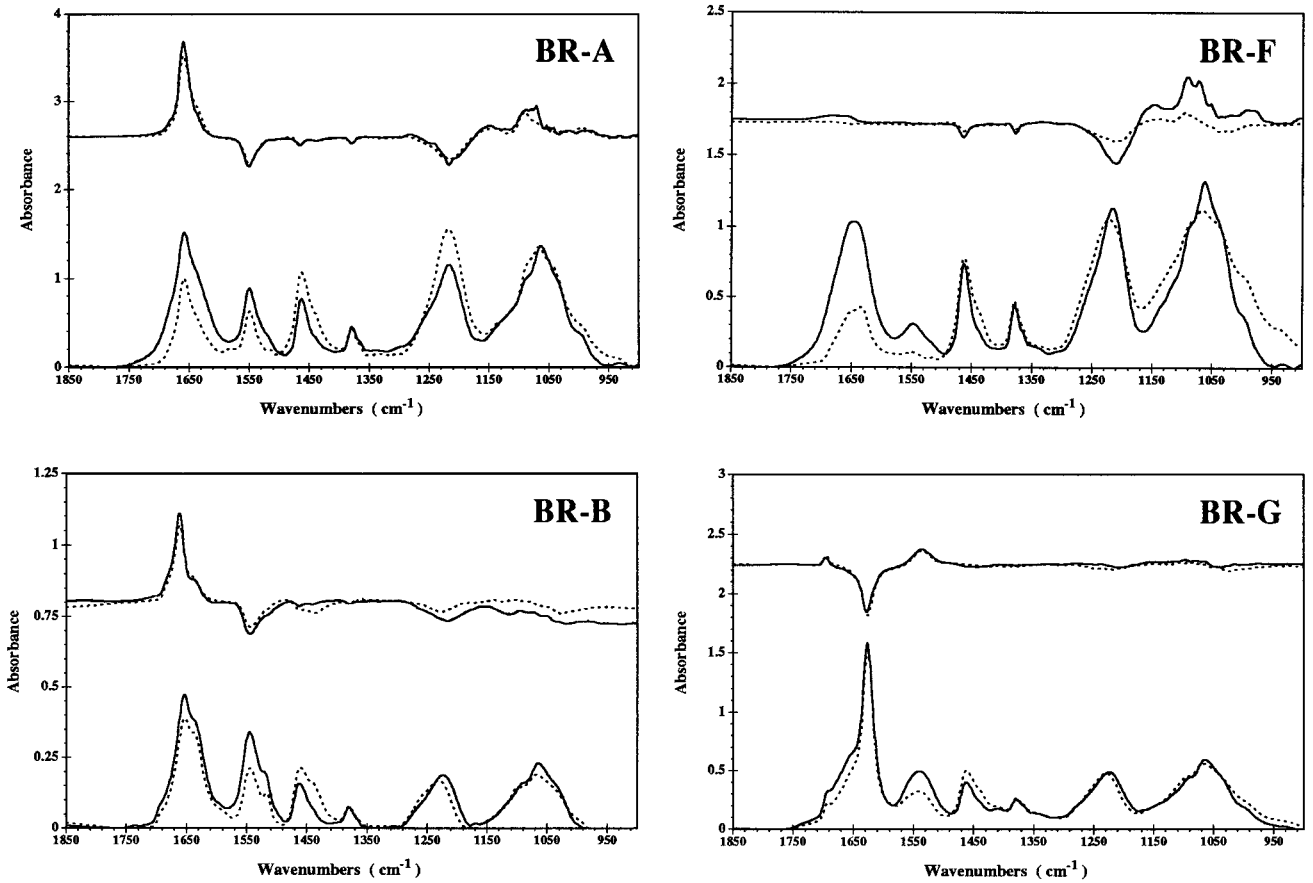

FIGURE 4: Amide exchange experiments on the individual BR helices in phospholipid multilayers. Spectra are shown for the samples in the presence of H_2O (solid lines) and after an extended period of exposure to D_2O (dotted lines). The film containing the BR-F peptide was exposed to D_2O continuously for 5 h, while the other films were exposed to D_2O continuously for at least 17 h. The lower traces in each panel represent absolute infrared absorbance spectra of the sample acquired with perpendicular polarization of the beam relative to the optical plane of incidence. The upper traces in each panel represent the corresponding polarized infrared difference spectra, *i.e.* parallel minus perpendicular, multiplied by a factor of 3. All of the spectra were acquired at an angle of incidence of 45° (relative to the plane of the sample substrate). Spectra derived from amide exchange experiments on samples containing the BR-D and BR-E peptides are shown in Figure S4 in the Supporting Information.

Table 1). Therefore, the oriented α-helices in the BR-A, BR-B, BR-D, and BR-E peptides and the oriented β-sheet in the BR-G peptide are all strongly resistant to H/D exchange, even after continuous exposure to deuterated solvent for time periods in excess of 16 h. These observations indicate that the bulk of the amide exchange observed in the absolute absorbance spectra of the BR peptides derives from regions of the polypeptide backbones that are not well-oriented relative to the phospholipid bilayer. A secondary structural element that is stably integrated in the phospholipid bilayer on the time scale of this experiment would be expected to retain a fully protonated polypeptide backbone (Zhang et al., 1992; Earnest et al., 1990; Holloway & Buchheit, 1990). Resistance to amide exchange does not prove that the secondary structural elements are integrated into the phospholipid bilayer because α-helices or β-sheets in a peripheral conformation could also be resistant to exchange, depending on their degree of thermodynamic stability (Englander & Mayne, 1992; Roder, 1989; Miranker et al., 1996). However, the observed dichroism of the BR-A, BR-B, BR-D, BR-E, and BR-G peptides in conjunction with their resistance to amide exchange support the hypothesis that the individual peptides form stable, transbilayer structures.

The quantitative analysis of the dichroism spectra (Table 1) suggests that there might be some degree of amide exchange of the oriented protein secondary structure (*i.e.* the estimated population of protected oriented protons is less than 100% for all of the peptides). However, there are potential inaccuracies in the integration of the dichroism spectra due to the low magnitude of the protein absorbance coupled with a small degree of uncertainty in the procedure used to scale the spectra before and after D_2O exchange. These effects are more severe and render the quantitation less reliable for samples with a high lipid-to-protein ratio, such as the samples of the BR-D peptide. In any event, it would be premature to conclude that there is exchange of the oriented secondary structure unless the appearance of dichroism at the position of deuterated amide bonds (approximately 1440 cm^{-1}) can be correlated with the disappearance of dichroism at the position of protonated amide bonds (approximately 1540 cm^{-1}). The only sample which unambiguously shows dichroism at the position of deuterated amide bonds is that of the BR-B peptide (Figure 4), which is the sample with the lowest lipid-to-protein ratio and also the highest degree of apparent exchange of its oriented secondary structure (Table 1). The shoulder on the amide II peak at 1525 cm^{-1} in the dichroism spectrum of the protonated BR-B sample completely disappears upon exposure to D_2O. This shoulder probably derives from the minor component of β-sheet structure that is oriented parallel to the membrane surface; the relatively rapid amide exchange observed for this structure is consistent with a peripheral location relative to the phospholipid bilayer as hypothesized

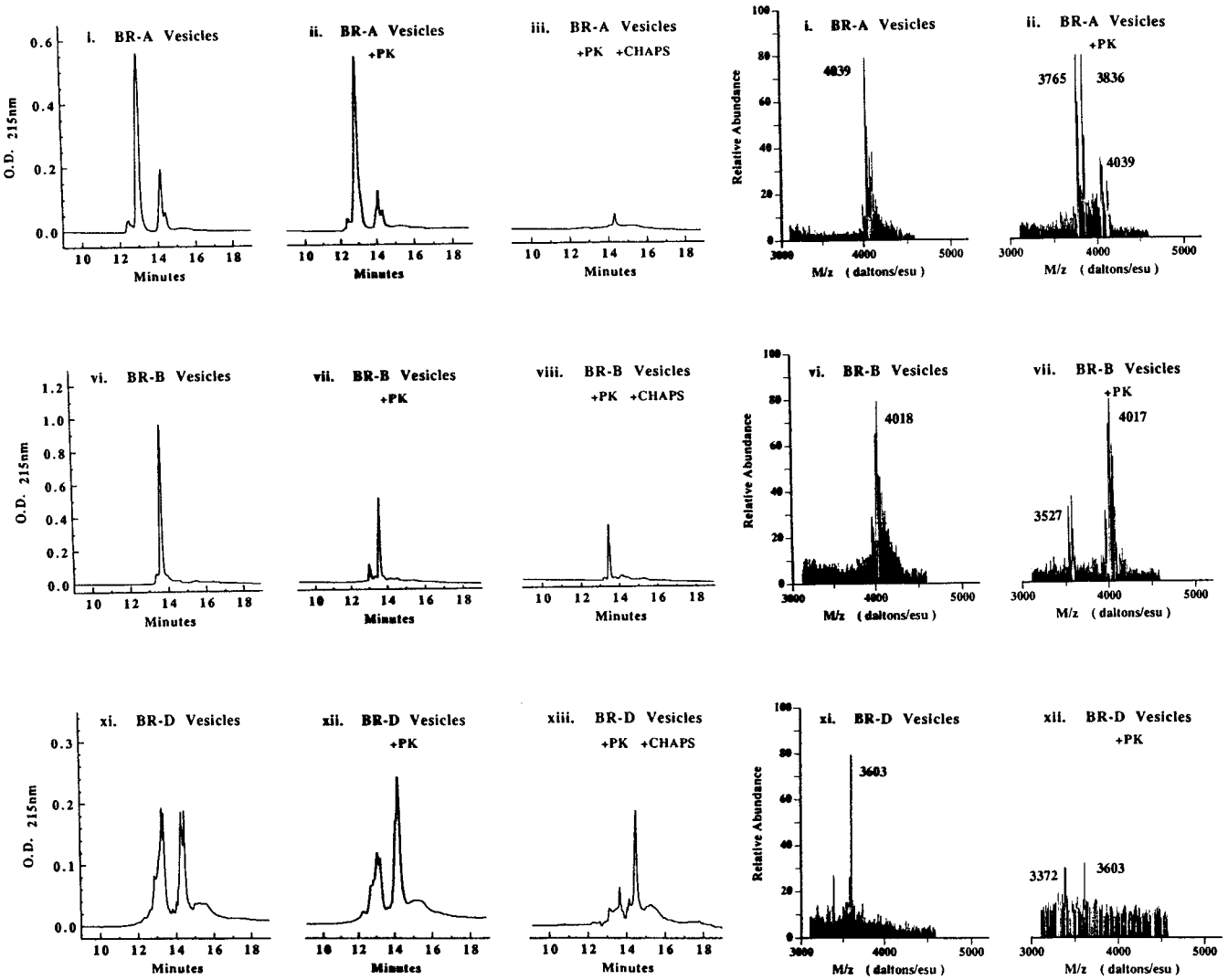

FIGURE 5: Molecular protease protection experiments on the individual BR helices in reconstituted phospholipid vesicles. Each row shows data for a single BR peptide (or for the pure *Halo*-lipid vesicle control). The first three columns show reversed phase HPLC traces for the vesicles incubated for 2.5 h at 37 °C under three conditions: minus proteinase K, plus proteinase K, and plus proteinase K plus CHAPS. The final two columns show deconvolved mass spectra of the principal peptide peaks from the samples with and without proteinase K treatment.

above. However, the magnitude of the principal amide II dichroism peak associated with the oriented α-helix in the BR-B sample is also reduced after exposure to D_2O, suggesting that some of this secondary structure has also experienced amide exchange during the experiment.

This effect could arise either from full exchange of the backbone protons on some fraction of peptide molecules or from partial exchange of a fraction of the backbone protons on all of the peptide molecules. Full exchange would certainly require ejection of the helix from the membrane, while partial exchange could occur by local conformational fluctuations involving the helix termini, for instance breathing motions of the final turn of the helix. In order to distinguish between these possibilities, an equivalent sample of the BR-B peptide was monitored over the course of several weeks, during which it was continuously exposed to D_2O. Following a similar reduction in the intensity of the oriented amide II absorbance during the first several hours of exposure to D_2O, the intensity of this band remained stable during the remainder of the time period (data not shown), leading us to conclude that the exchange of the oriented α-helical structure in the BR-B peptide probably arises from breathing motions of the helix termini.

Molecular Protease Protection Experiments on Vesicles in Solution. The results of protease protection experiments conducted on the vesicles containing the BR fragments are shown in Figure 5 (and summarized in Table 1 as well as the schematic diagram in Figure 1). Proteinase K was used for these experiments because it is a nonspecific endoprotease, *i.e.* its cleavage rate is largely independent of the polypeptide sequence (Whittaker et al., 1994). Furthermore, prior to incubation at 37 °C, several freeze−thaw cycles were performed in order to give the protease equal access to both the external volume and the lumen of the vesicles. Therefore, in order to be protected from proteolytic digestion in these experiments, peptide bonds must be chemically sequestered either within the protective barrier of the phospholipid bilayer or in some kind of stable protein structure (Dumont et al., 1985; Audigier et al., 1987; Rietveld et al., 1986; Anderson et al., 1982). These experiments provide a useful complement to the amide exchange experiments because they provide information on the conformational stability of the peptide molecules in the vesicles free in solution rather than after deposition as protein/phospholipid multilayers. The results of the protease digestion reactions were analyzed initially by reversed phase chromatography, and the material

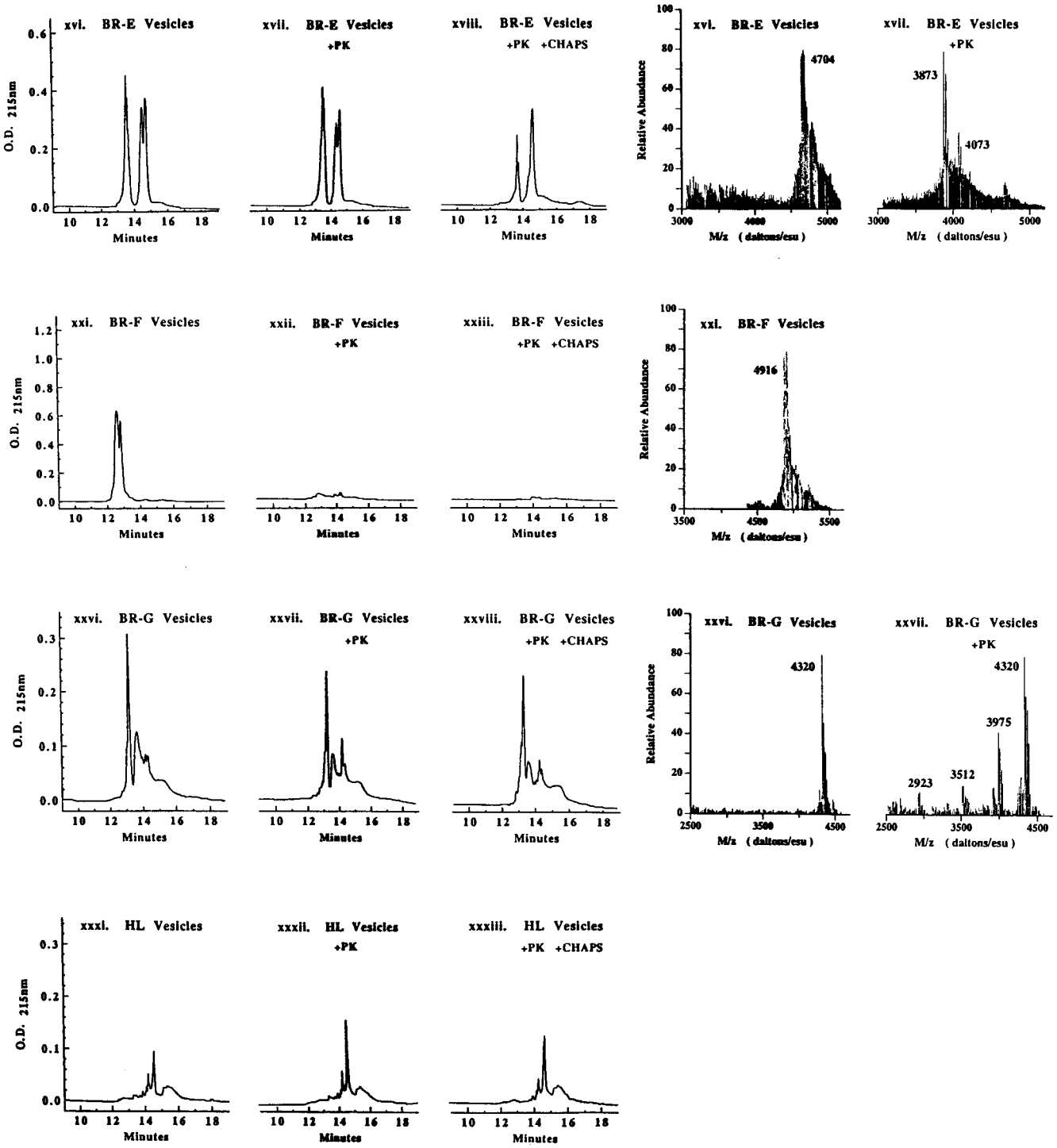

FIGURE 5: (CONTINUED)

eluted from the column was subsequently analyzed by fast atom bombardment mass spectrometry (FAB-MS). This technique determines of the mass of the protected peptide fragments within approximately ±2 atomic mass units, allowing the exact site of the protease attack to be inferred in most cases. Control reactions were conducted in which the vesicles were incubated in the absence of proteinase K, and additional reactions were conducted in which the vesicles were solubilized in the nonionic detergent CHAPS prior the initiation of the proteolysis reaction.

Two points deserve clarification relative to the interpretation of the chromatograms in Figure 5. First, because of the different lipid-to-protein ratios in the samples as well as variations in the extinction coefficients of the peptides at 215 nm, the traces show substantial variations in the relative intensity of the peptide-derived peak(s) compared to the phospholipid-derived and protease-derived peaks. Second, examination of the chromatograms reveals that some of the peptides give rise to multiple chromatographic peaks, even in the absence of added protease. The control sample of the BR-G peptide produces three peaks, while the control samples of the BR-A, BR-D, and BR-E peptides produce two peaks. Mass spectra of all three BR-G peaks look identical (Table 1), indicating that the different species must represent different conformations or different oligomeric states of the same polypeptide. Intact bacteriorhodopsin produces two peaks when run on the same column in this solvent system, with the second peak representing a noncovalent oligomer (Hunt, 1993). The mass spectra of the second peak in the control samples of BR-D indicate the

presence of a 29-residue fragment, presumably derived from a low level of spontaneous proteolysis in these vesicles. In the case of the control samples of the BR-A and BR-E peptides, the initial peak in the chromatogram unambiguously contains the pristine polypeptide, but we had difficulty identifying the polypeptide species in the second peak using mass spectrometry. We believe that the second peak probably comprises non-covalent oligomers of the pristine polypeptide but cannot exclude the possibility that it also includes some spontaneously proteolyzed species.

The results of the protease protection experiments parallel those of the amide exchange experiments, showing that the BR-A, BR-B, BR-D, BR-E, and BR-G peptides are all strongly protected from digestion by proteinase K. The F peptide, on the other hand, is quantitatively digested even at the earliest time point that was measured (2.5 h). Figure 5 shows data obtained using vesicles containing the BR-F peptide at a 1:1 weight ratio of lipid-to-protein; identical results were obtained with vesicles containing a 13:1 weight ratio of lipid-to-protein (data not shown). These data support the conclusion from the amide exchange experiment that the BR-F peptide does not form any stable secondary structure in association with the *Halo*-lipid vesicles under the conditions explored in these experiments.

Although the other five peptides all show substantial resistance to proteolysis, the magnitude of the resistance varies considerably (Figure 5). For instance, the BR-A peptide is almost completely resistant to proteolysis during a 2.5 h incubation, while the BR-B peptide is approximately 50% digested during the same time period. The BR-G peptide shows an intermediate level of protease resistance. Partial protease protection could reflect the slow degradation of a single, uniform peptide population, or it could reflect the existence of more than one conformational state in the peptide population. Longer digestions of both the BR-B and BR-G peptides show continuing proteolysis at approximately the same rate (data not shown), suggesting that a uniform population is being digested at a slow rate. The relative rate of proteolysis of the peptides is different in the presence of the nonionic detergent CHAPS than in the intact vesicles. For example, the BR-A peptide is quantitatively digested in the presence of the detergent even though it is the most strongly protected peptide in the lipid bilayer. The BR-B peptide, on the other hand, is substantially protected in the presence of the detergent, even though it is susceptible to slow proteolysis in the lipid bilayer. Presumably these differences reflect the relative stability of the peptide secondary structure in the different amphiphilic environments.

Figure 1 shows the locations of the proteolytic cleavage sites in the individual BR peptides as identified in a detailed analysis of the mass spectrometry data (Table 1). While the termini of all of the protected peptides are actively digested by the protease in these experiments, a very limited spectrum of proteolysis products is observed. Focusing attention first on the α-helical polypeptides, we note that there is virtually no pristine polypeptide remaining in the BR-A and BR-E vesicles following exposure to proteinase K; these peptides are almost quantitatively converted to species 35 and 32 residues in length, respectively (Figure 5 and Table 1). The principal proteolysis products of the BR-B and BR-D peptides are 32 and 33 residues in length, respectively. Including the capping structures at the helix termini, the corresponding α-helices observed in the native structure of BR are only 25−28 residues in length (Grigorieff et al., 1996), with the regular secondary structure comprising 23−25 residues. Thus, the protease protection conferred by the bilayer extends beyond the ends of the stable tertiary structure in the native protein molecule. Moreover, even in the flanking sequences, cleavage is observed only at a limited number of the potential sites, indicating some source of sequence specificity in the proteolytic reaction. Because this specificity is unlikely to derive from the substrate specificity of the protease, the restricted pattern of cleavage is likely to reflect either structural specificity in the tight association of the flanking sequences with the headgroup region of the phospholipid bilayer and/or conformational destabilization of the transbilayer α-helix following cleavage at specific combinations of individual sites.

The fact that we do not observe any proteolysis product smaller than 23 residues in length for any of the peptides suggests that the membrane-spanning region of the peptides is digested by the protease in an all-or-none fashion. For example, while the BR-B and BR-D peptides are partially protected from proteolysis in association with the phospholipid vesicles, quantitation of the peak areas in the corresponding chromatograms shows that more of the peptide bonds in these molecules have been digested than can be accounted for by the proteolytic removal of their termini. Our failure to detect smaller peptide fragments in these samples suggests that some fraction of the peptide molecules have been completely degraded by the protease. Because the protected peptide fragments observed in high yield are longer than the corresponding transmembrane helices, it seems likely that reduction of the length of the flanking sequences below a critical limit destabilizes the transmembrane conformation of the peptide (Dumont et al., 1985), which would render the peptide sensitive to proteolysis by pushing its conformational equilibrium toward peripherally membrane-bound and therefore protease-sensitive conformations (*e.g.* conformations similar to that observed for the pristine BR-F peptide in our experiments). In this context, it is noteworthy that the transmembrane helix with the shortest flanking sequence exhibits the greatest degree of protease sensitivity. Compared to the helix observed in the native structure of BR, the BR-B peptide contains an amino-terminal flanking sequence only two residues in length, substantially shorter than that at either terminus of any of the other α-helical peptides (Figure 1). In addition to showing the highest rate of digestion by proteinase K of any of these peptides, BR-B is the only peptide showing any detectable amide exchange of the oriented α-helical secondary structure, providing experimental evidence that there is some degree of conformational instability in the transmembrane region of this α-helix.

The mass spectra of the BR-G vesicles following exposure to proteinase K show that the major proteolysis product of this peptide is 37 residues in length, *i.e.* four residues shorter than the pristine polypeptide. Both this fragment and the pristine polypeptide are strongly resistant to proteolysis. Such resistance would be expected if the peptide were stably integrated into the phospholipid bilayer but could also be attributable to the formation of a very stable structure in an aqueous environment. As indicated in Figure 1 and Table 1, a variety of smaller proteolytic fragments are also observed for the BR-G peptide, although at yields substantially lower than that of the 37-residue fragment. Combining the observed locations of the low-frequency cleavage sites with

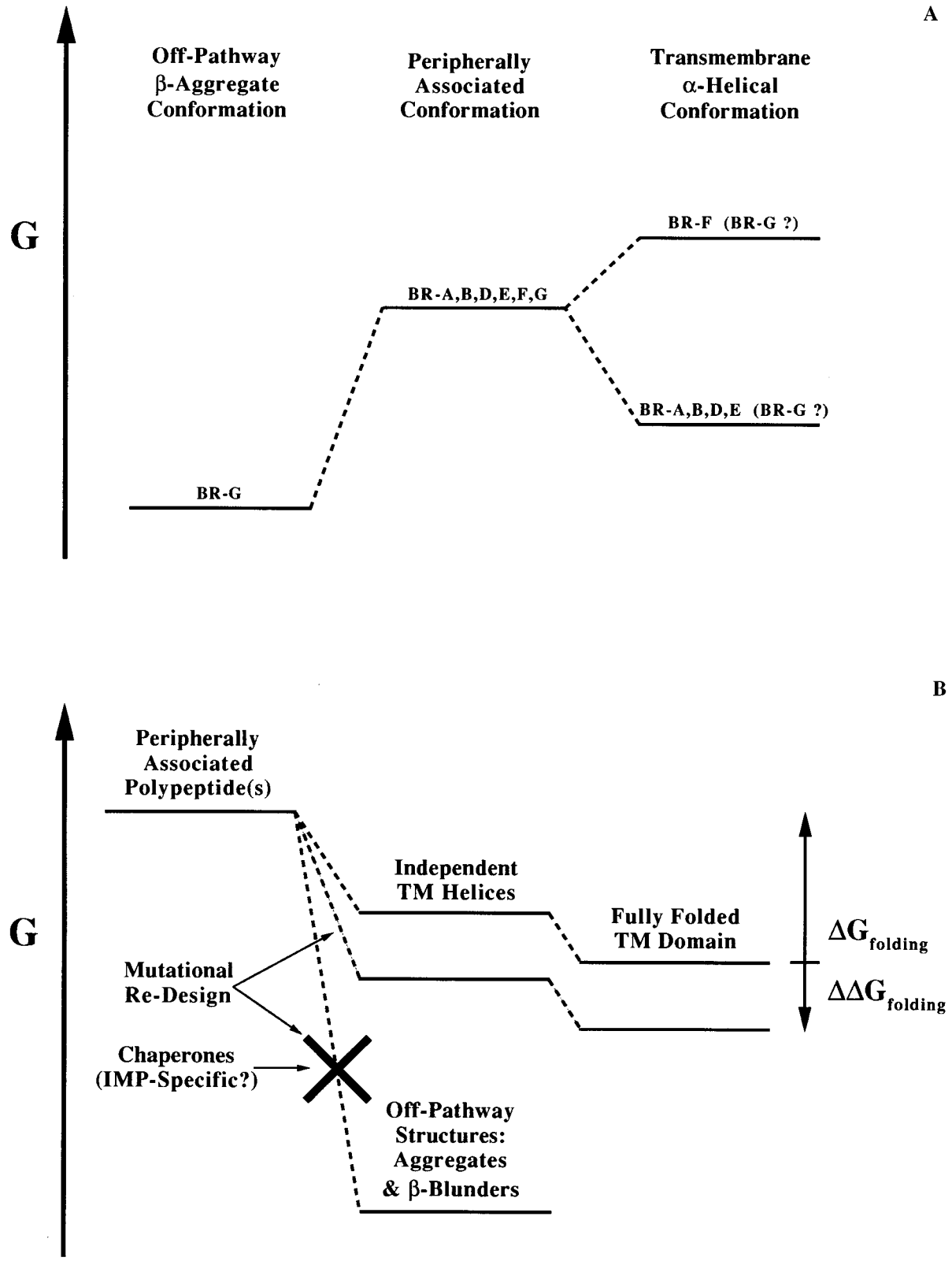

FIGURE 6: Schematic summary of qualitative thermodynamic conclusions. (A) Relative thermodynamic stability of the six BR fragments as deduced from the experiments presented in this paper. (B) Scheme for the thermodynamic re-engineering of integral membrane protein stability.

the results of Chou−Fasman analysis (Fasman & Chou, 1978), we believe that the segments from gly-5 to leu-9, glu-12 to asp-20, and leu-29 to arg-33 are reasonable candidates to form β-strands.

DISCUSSION

Assuming that the synthetic peptides have reached thermodynamic equilibrium in the *Halo*-lipid vesicles used in our experiments, the results that we present in this paper can be interpreted as a qualitative study of the relative thermodynamic stability of the membrane-associated conformations of the bacteriorhodopsin peptides (Figure 6A). On this basis, we would conclude that a transmembrane α-helical conformation is more stable than any peripherally membrane-bound conformation for the BR-A, BR-B, BR-D, and BR-E peptides [and for the BR-C peptide at pH < 6,

as shown in Hunt et al. (1997)]. In contrast, we would conclude that a peripherally membrane-bound conformation (Jacobs & White, 1989; White & Wimley, 1996) is more stable than a transmembrane α-helical conformation for the BR-F peptide. The enigmatic observation of a hyperstable *β*-sheet conformation for the BR-G peptide would indicate that this conformation is more stable than any other membrane-associated conformation of the peptide, but the resulting dominance of this conformation in the peptide population prevents us from assessing the relative stability of the transmembrane α-helical and peripherally membrane-bound conformations of this peptide (Figure 6A).

While it is difficult to verify the assumption that the synthetic BR peptides have reached thermodynamic equilibrium in the reconstituted vesicles, the K^+-SDS reconstitution protocol that we employed in preparing our samples makes it unlikely that we would have failed to observe a transbilayer α-helix if a peptide were stable in this conformation. Following K^+-mediated precipitation of the SDS, a relatively high concentration of detergent remains in the phospholipid bilayers (Popot et al., 1987); this residual detergent is removed from the bilayers gradually during a subsequent dialysis step. Due to the high detergent content, the permeability barrier of the bilayer should be negligible at the outset of the dialysis period and then gradually increase to normal levels (Popot et al., 1987). We expect the peptides to have ample opportunity to adopt their equilibrium conformation during this dialysis period. More importantly, there is direct experimental evidence that this kind of conformational equilibration takes place. Starting with intact BR dispersed in SDS where there should be no significant interaction between the different helices, the K^+-SDS reconstitution protocol leads to efficient regeneration of native BR (Popot et al., 1987). Thus, in the context of the intact protein, the individual helices are clearly capable of achieving their equilibrium conformation relative to the phospholipid bilayer during the course of the K^+-SDS reconstitution protocol. We conclude that it is likely that the most stable bilayer-associated peptide conformation is observed in our samples.

Although our results provide insight into the relative free-energy of different conformational states, it is important to note that we cannot quantitate these differences using experiments of the type presented in this paper. We have shown that the BR-G peptide forms a stable membrane-associated *β*-sheet structure as assayed by amide exchange and protease protection experiments. Although we believe that we could have detected a 10% population of transbilayer helices in the BR-G samples, we could not have detected a 1% population. Thus, the transbilayer α-helical conformation of the BR-G peptide could lie within 3 kcal/mol of the *β*-sheet conformation, and we would not have been able to detect it in our experiments. Similar considerations apply to our observations with the BR-F peptide. While our experiments suggest that a peripheral conformation lacking stable secondary structure is the lowest energy conformation of this peptide in *Halo*-lipid membranes, we have not quantitated the relative free energy of the transbilayer α-helical conformation of the peptide and can only say that it is likely to be at least 1.5 kcal/mol higher in free energy than the observed conformation.

Combining the results presented in this paper with those presented in Hunt et al. (1997), we have shown that the five N-terminal α-helices observed in the native tertiary structure of BR are capable of forming stable transbilayer α-helices in isolation from the remainder of the tertiary structure of BR. Thus, the folding of the amino terminus of this polytopic integral membrane protein could proceed by a simple mechanism in which individually stable transmembrane α-helices are inserted into the bilayer in the first stage of the folding pathway (Popot & Engelman, 1990). The results reported in Hunt et al. (1997) also show that the C-helix of BR is capable of inserting into the phospholipid bilayer spontaneously. If the other four helices at the amino terminus of BR share this property, the folding of this portion of the protein molecule would be expected to proceed spontaneously and efficiently.

However, the two C-terminal α-helices in BR do not form stable transbilayer helices in our assays, suggesting that the folding of the carboxy terminus of BR may be more complicated. Because the F and G helices of BR are covalently linked in the protein molecule and the carboxy terminus of the G helix is cytoplasmic, topological contraints would force the F and G helices to insert in tandem (unless the entire protein is first secreted to the periplasm). In this context, it is likely that the F and G helices of BR interact with one another during insertion into the membrane, potentially by forming a stable α-helical hairpin (Engelman & Steitz, 1981). Therefore, we investigated whether there was any evidence of an interaction between the corresponding peptides in phospholipid vesicles. Samples were produced both by reconstituting the peptides in tandem and by fusing the vesicles containing the individual peptides. There was no evidence of altered conformational properties in any of these experiments, and, in particular, there was never any sign of transmembrane α-helical structure in polarized FTIR spectra of multilayers containing the polypeptides corresponding to both the F and G helices of BR (data not shown). An important issue to be addressed in future work is whether a covalent link between F and G would cause them to exhibit different conformational properties.

In spite of this complication, the qualitatively different conformational properties exhibited by the isolated α-helices from the amino *vs* carboxy termini of BR suggest that the folding of the carboxy terminus may involve a somewhat more elaborate mechanism than that envisioned by the two-stage model of integral membrane protein folding. One possibility is that the F and G helices interact with other regions of the protein molecule prior to their insertion into the membrane. (Conceivably, the cleaved N-terminal signal sequence of BR could even participate in facilitating these interactions, but such participation cannot be an obligate step in the assembly pathway because mature BR can refold to the native state in the absence of its signal sequence.) Alternatively, the F and G helices could insert into the membrane following the formation of a binding site within the membrane by the five amino-terminal α-helices of BR (Popot et al., 1987; Booth et al., 1995, 1996). This mechanism would be consistent with the observation that there is a rate-limiting protein conformational change that precedes retinal binding during the regeneration of photoactive BR from two chymotryptic fragments.

Whatever the detailed explanation for this behavior, it is possible that a similar pattern holds for the relative transmembrane stability of the N-terminal *vs* C-terminal α-helices in other polytopic IMP's. Observations with the lactose permease from *E. coli* indicate that it is possible to stably express *in vivo* N-terminal fragments but not C-terminal

fragments containing a subset of the transmembrane α-helices in the intact protein molecule (Sahin-Toth et al., 1996). These observations would be consistent with the N-terminal but not C-terminal α-helices integrating stably into the bilayer on their own. Potentially, efficient folding *in vivo* depends on rapid and stable membrane integration of the segments that are synthesized first so that they can serve as a folding template for the distal segments; in this case, evolution would select for a C-terminal location for α-helices which have a lower intrinsic stability in the transmembrane conformation due to functional constraints (Rothschild et al., 1989).

As an initial attempt to gain insight into the sequence-dependent contributions to the stability of transbilayer α-helices, we can ask why the BR-F peptide fails to form such a structure while other peptides with similar overall hydrophobicity do (*e.g.* BR-C and BR-D). One possible explanation is that the hydrophobic core of this sequence is shorter than that of any of the other BR peptides (Figure 1). Another possible explanation concerns the steric bulk on one side of the F helix. Specifically, two tryptophan residues and one tyrosine residue all line up on the same face of the α-helix on three successive turns. These residues form an aromatic box around the retinal chromophore in the native structure of BR (Rothschild et al., 1989; Grigorieff et al., 1996). It is possible that steric crowding of these side chains could destabilize the α-helical conformation of the polypeptide backbone or that insertion of this large steric bulk into the core of the bilayer could destabilize the transbilayer configuration of the helix. Further investigations will be required to establish the correct explanation for the failure of the BR-F peptide to form a stable transbilayer α-helix; the experiments described in this paper provide a number of convenient assays which could be applied to such investigations.

The observation that the BR-G peptide forms a stable β-sheet structure is enigmatic. Several lines of evidence indicate that it is extremely unlikely that this segment of the polypeptide chain adopts a β-sheet conformation in the native tertiary structure of BR (Glaeser et al., 1991). First, the high-resolution electron density map of BR shows well-defined α-helical structure in this region of the protein structure (Grigorieff et al., 1996). Second, polarized FTIR spectroscopy of intact BR does not show any evidence of β-structure with the kind of orientation relative to the membrane plane observed in the samples of the BR-G peptide (Earnest et al., 1990; Earnest, 1987). Finally, polarized FTIR spectroscopy of a chymotryptic fragment of BR containing helices C through G, a fragment which is also competent in regeneration of the native structure of BR, shows no evidence of the type of β-structure exhibited by the BR-G peptide (Earnest, 1987). Thus, the sequence corresponding to the G helix in BR seems to be capable of adopting radically different conformations in different molecular contexts, and the isolated peptide seems to adopt a very stable conformation which is not on the folding pathway of the parental protein molecule (Hartl, 1996; Kelly, 1996).

Most of the hydrophobic amino acids commonly found in transmembrane α-helices (*i.e.* tyr, val, ile, trp, phe, and leu) have a higher propensity to form β-strands than α-helices according to the scale of Chou and Fasman derived from the statistical analysis of observed secondary structure in soluble proteins (Fasman & Chou, 1978). However, an experimental study of α-helix formation in SDS micelles has shown that α-helical propensity in a hydrophobic environment scales with the hydrophobicity of the amino acid side-chain and not according to the structural propensity of the residue in soluble proteins (Li & Deber, 1994). Thus, Chou−Fasman analysis predicts the formation of β-structure by all of the BR peptides, especially the BR-D, BR-F, and BR-G peptides, but the efficient formation of a stable β-sheet structure is observed only for the BR-G peptide, indicating that this conformational preference is a unique property of the BR-G sequence and not determined simply by the secondary structural propensity of the constituent amino acids.

The experiments that we have performed fall short of establishing a transmembrane structure for the BR-G peptide. The hyperstable β-structure adopted by the BR-G peptide is reminiscent of the amyloid structures formed by the aggregation of some proteins (Kelly, 1996); however, there is no reason to expect an amyloid aggregate to be efficiently incorporated in phospholipid membranes or to adopt a well-defined orientation relative to the plane of the bilayer in those membranes. Nonetheless, we cannot exclude the possibility of a surface-associated β-sheet exhibiting strong protease resistance or of some kind of unusual lipoprotein aggregate. On the other hand, the BR-G peptide does exhibit all of the biochemical and spectroscopic properties anticipated for a transmembrane β-sheet. In addition to showing spectral features at the appropriate frequencies and with the appropriate orientation relative to the bilayer plane, the peptide bonds are highly resistant to hydrogen/deuterium exchange and to digestion by proteases in the aqueous phase. Further investigations will be required to establish the exact nature of the β-sheet structure formed by the BR-G peptide. If the structure is transmembrane, it is likely that the peptide forms an oligomer because it is too small to form a membrane-spanning β-barrel structure on its own, and an extended β-sheet is believed to be unstable in a transmembrane configuration (Engelman & Steitz, 1981). In SDS polyacrylamide gel electrophoresis, the peptide shows a mixture of a species migrating at the monomer molecular weight and large aggregates (data not shown); however, we do not have any experimental data on the aggregation state of the BR-G peptide in phospholipid vesicles. Although the structure adopted by the BR-G peptide represents an obstacle to the proper folding of BR, it is possible that this structure could be used productively in some other biological context given its extreme stability.

The studies presented in this paper and the accompanying paper (Hunt et al., 1997) represent an initial step toward developing an experimentally-based understanding of the thermodynamics of integral membrane protein structure and assembly. We believe that these results also provide insight into potential roles for molecular chaperones in assisting the assembly of integral membrane proteins *in vivo* (Figure 6B). Extensive studies on the spontaneous and chaperone-assisted folding of soluble proteins have made it clear that one of the major functions of the chaperones is to deal with the kinetic and thermodynamic problems encountered on the spontaneous folding pathway (Hubbard & Sander, 1991; Jackson et al., 1993; Todd et al., 1996; Hartl, 1996). The conformational properties of the F and G helices represent obvious thermodynamic problems relative to the assembly of BR. Cells must be able to surmount conformational problems of the type presented by these helices in order to achieve efficient folding and assembly of integral membrane proteins; it is reasonable to expect that molecular chaperones

might be involved in this process, possibly even chaperones that are optimized for the folding of integral membrane proteins and whose existence has yet to be elucidated.

For example, the stable off-pathway β-sheet structure formed by the BR-G peptide would represent a major obstacle to either the folding or degradation of newly synthesized BR (Kelly, 1996). It would be sensible for cells to employ a molecular chaperone either to prevent the formation of this structure or to disaggregate it once formed. Turning attention to the conformational problem posed by the BR-F helix, a hydrophobic polypeptide that fails to adopt any stable structure is likely to have a strong propensity to aggregate. We were surprised that the BR-F peptide did not exhibit any detectable tendency to aggregate in our samples, and this observation suggests that the phospholipid bilayer itself may serve the role of a conformational chaperone for hydrophobic polypeptides. However, it is not clear whether this activity would be adequate to safeguard the conformational integrity of this sequence *in vivo* given the immense spectrum of aggregation-prone species in a cell (Kurada & O'Tousa, 1995), and it seems possible that a molecular chaperone could also play a role in protecting helices of this kind that do not adopt a stable transmembrane conformation on their own prior to the complete assembly of the transmembrane domain.

The peptidyl-prolyl *cis*−*trans* isomerase NinaA has been shown to be required for efficient biosynthetic assembly of rhodopsin in *Drosophila melanogaster* photoreceptor cells (Baker et al., 1994; Schmid, 1995). In this context, it is possible that the conformational problems with the BR-F and BR-G helices could derive from an inappropriate proline isomerization state in the peptides. [The BR-F helix contains pro-186, which has been implicated in the protein conformational changes that occur during the BR photocycle (Ludlam et al., 1995)]. However, this explanation seems somewhat unlikely because α-helices are formed using the thermodynamically favored *trans* isomer of proline (Stein, 1993), and the BR-B and BR-C peptides, which both have proline residues in their transmembrane α-helices, efficiently adopt their native conformation in our assays.

If the two-stage model of IMP folding were correct in detail, α-helical integral membrane proteins would be expected to fold spontaneously and with great efficiency to a stable native state both *in vitro* and *in vivo*. However, to date, bacteriorhodopsin is the only polytopic α-helical integral membrane protein to have been successfully refolded from a denatured state *in vitro* (Liao et al., 1984; Huang et al., 1981; Popot et al., 1987; Booth et al., 1996). Furthermore, IMP's have proven to be exceedingly difficult to over-produce *in vivo* (Grisshammer & Tate, 1995), and the limited conformational stability of IMP's is a chronic and daunting problem in their biochemical manipulation (Garavito et al., 1996). An important question to be addressed in future work is whether there is a positive correlation between the ease of re-folding an α-helical IMP, its thermodynamic stability in the native state, and the stability of its constituent α-helices in the transmembrane conformation. Simple thermodynamic considerations suggest that such a correlation should exist because the free energy of the intermediate states along the reaction coordinate of a complex assembly process should be one determinant of the free energy of the final state (Figure 6B). If such a correlation does exist, we can foresee a simple scheme for the "thermodynamic engineering" of polytopic α-helical IMP's. Specifically, it could be possible to improve the folding properties and the overall thermodynamic stability of the intact protein by improving the thermodynamic stability of the individual constituent α-helices in the transmembrane conformation (Figure 6B). In this case, the assays used in this paper could be applied to evaluate the thermodynamic effect of individual mutations on model peptides. More importantly, once the general principles determining the stability of isolated α-helices are established in more detail, it would be possible to apply the technique to any IMP with a known sequence, even at the earliest stages of an expression project and prior to the availability of any biochemical material.

ACKNOWLEDGMENT

The authors acknowledge Jim Elliot for chemical synthesis and purification of the BR peptides and Walt McMurray and Giuseppe Giordano for performing the mass spectral analyses. We also thank Paula Booth, Mischa Machius, and Philip Thomas for critical reviews of the manuscript.

SUPPORTING INFORMATION AVAILABLE

A complete set of CD and FTIR spectra for the BR-D and BR-E vesicles plus dichroism plots (quantitating the variation of the dichroic ratio as a function of sample tilt angle) for a set of protein and lipid absorbances in all of the samples shown in Figure 3 (6 pages). See any current masthead page for ordering and access information.

REFERENCES

Anderson, D. J., Walter, P., & Blobel, G. (1982) *J. Cell Biol. 93*, 501.
Anfinsen, C. B. (1973) *Science 181*, 223.
Audigier, Y., Friedlander, M., & Blobel, G. (1987) *Proc. Natl. Acad. Sci. U.S.A. 84*, 5783.
Baker, E. K., Colley, N. J., & Zuker, C. S. (1994) *EMBO J. 13*, 4886.
Baldwin, J. M., Henderson, R., Beckman, E., & Zemlin, F. (1988) *J. Mol. Biol. 202*, 585.
Batenburg, A. M., Hibbeln, J. C., Verkleij, A. J., & de Kruijff, B. (1987) *Biochim. Biophys. Acta 903*, 142.
Blobel, G. (1980) *Proc. Natl. Acad. Sci. U.S.A. 77*, 1496.
Booth, P. J., Flitsch, S. L., Stern, L. J., Greenhalgh, D. A., Kim, P. S., & Khorana, H. G. (1995) *Nat. Struct. Biol. 2*, 139.
Booth, P. J., Farooq, A., & Flitsch, S. L. (1996) *Biochemistry 35*, 5902.
Brasseur, R. (1991) *J. Biol. Chem. 266*, 16120.
Büldt, G., Gally, H. U., Seelig, J., & Zaccaï, G. (1979) *J. Mol. Biol. 134*, 673.
Cantor, C. R., & Schimmel, P. R. (1980) in *Biophysical Chemistry, Part II: Techniques for the Study of Biological Structure and Function*, W. H. Freeman, San Francisco.
Casal, H. L., & Mantsch, H. H. (1984) *Biochim. Biophys. Acta 779*, 381.
Challou, N., Goormaghtigh, E., Cabiaux, V., Conrath, K., & Ruysschaert, J. M. (1994) *Biochemistry 33*, 6902.
Chirgadze, Y. N., & Nevskaya, N. A. (1976) *Biopolymers 15*, 607.
Clark, N. A., Rothschild, K. J., Luippold, D. A., & Simon, B. A. (1980) *Biophys. J. 31*, 65.
Dempsey, C. E., Bazzo, R., Harvey, T. S., Syperek, I., Boheim, G., & Campbell, I. D. (1991) *FEBS Lett. 281*, 240.
Dobson, C. M. (1994) *Curr. Biol. 4*, 636.
Dumont, M. E., Trewhella, J., Engelman, D. M., & Richards, F. M. (1985) *J. Membr. Biol. 88*, 233.
Earnest, T. N. (1987) in *Fourier Transform Infrared and Resonance Raman Spectroscopic Studies of Bacteriorhodopsin*, Ph.D. Dissertation, Boston University, Boston, MA.
Earnest, T. N., Roepe, P. D., Braiman, M. S., Gillespie, J., & Rothschild, K. J. (1986) *Biochemistry 25*, 7793.

Earnest, T. N., Herzfeld, J., & Rothschild, K. J. (1990) *Biophys. J. 58*, 1539.
Ellis, R. J. (1994) *Curr. Biol. 4*, 633.
Engelman, D. M., & Steitz, T. A. (1981) *Cell 23*, 411.
Engelman, D. M., Steitz, T. A., & Goldman, A. (1986) *Annu. Rev. Biophys. Biophys. Chem. 15*, 321.
Englander, S. W., & Mayne, L. (1992) *Annu. Rev. Biophys. Biomol. Struct. 21*, 243.
Fasman, G. D., & Chou, P. (1978) *Adv. Enzymol. 47*, 45.
Fersht, A. R. (1993) *FEBS Lett. 325*, 5.
Fraser, R. D. B., & MacRae, T. P. (1973) in *Conformation in Fibrous Proteins and Related Synthetic Polypeptides*, Academic Press, New York.
Garavito, R. M., Picot, D., & Loll, P. J. (1996) *J. Bioenerg. Biomembr. 28*, 13.
Georgopoulos, C., & Welch, W. J. (1993) *Annu. Rev. Cell Biol. 9*, 601.
Glaeser, R. M., Downing, K. H., & Jap, B. K. (1991) *Biophys. J. 59*, 934.
Grigorieff, N., Ceska, T. A., Downing, K. H., Baldwin, J. M., & Henderson, R. (1996) *J. Mol. Biol. 259*, 393.
Grisshammer, R., & Tate, C. G. (1995) *Q. Rev. Biophys. 28*, 315.
Hartl, F. U. (1996) *Nature 381*, 571.
Helenius, A., & Simons, K. (1975) *Biochim. Biophys. Acta 415*, 29.
Henderson, R., Baldwin, J. M., Ceska, T. A., Zemlin, F., Beckmann, E., & Downing, K. H. (1990) *J. Mol. Biol. 213*, 899.
Holloway, P. W., & Buchheit, C. (1990) *Biochemistry 29*, 9631.
Huang, K. S., Bayley, H., Liao, M. J., London, E., & Khorana, H. G. (1981) *J. Biol. Chem. 256*, 3802.
Hubbard, T. J., & Sander, C. (1991) *Protein Eng. 4*, 711.
Hunt, J. F. (1993) in Biophysical Studies of Integral Membrane Protein Folding, Ph.D. Thesis, Yale University, New Haven, CT.
Hunt, J. F., Rath, P., Rothschild, K. J., & Engelman, D. M. (1997) *Biochemistry 36*, 15177−15192.
Jackson, G. S., Staniforth, R. A., Halsall, D. J., Atkinson, T., Holbrook, J. J., Clarke, A. R., & Burston, S. G. (1993) *Biochemistry 32*, 2554.
Jacobs, R. E., & White, S. H. (1989) *Biochemistry 28*, 3421.
Johnson, W. C., Jr. (1988) *Annu. Rev. Biophys. Biophys. Chem. 17*, 145.
Johnson, W. C., Jr. (1990) *Proteins 7*, 205.
Jordi, W., de Kroon, A. I., Killian, J. A., & de Kruijff, B. (1990) *Biochemistry 29*, 2312.
Kalghatgi, K., & Horváth, C. (1987) *J. Chromatogr. 398*, 335.
Kates, M., Kushwaha, S. C., & Sprott, G. D. (1982) *Methods Enzymol. 88*, 98.
Kelly, J. W. (1996) *Curr. Opin. Struct. Biol. 6*, 11.
Kleffel, B., Garavito, R. M., Baumeister, W., & Rosenbusch, J. P. (1985) *EMBO J. 4*, 1589.
Kleinschmidt, J. H., & Tamm, L. K. (1996) *Biochemistry 35*, 12993.
Krimm, S., & Abe, Y. (1972) *Proc. Natl. Acad. Sci. U.S.A. 69*, 2788.
Krimm, S., & Bandekar, J. (1986) *Adv. Protein Chem. 38*, 181.
Kuhlbrandt, W. (1988) *Q. Rev. Biophys. 21*, 429.
Kuhlbrandt, W. (1992) *Q. Rev. Biophys. 25*, 1.
Kumamoto, C. A. (1991) *Mol. Microbiol. 5*, 19.
Kurada, P., & O'Tousa, J. E. (1995) *Neuron 14*, 571.
Kyte, J., & Doolittle, R. F. (1982) *J. Mol. Biol. 157*, 105.
Li, S. C., & Deber, C. M. (1994) *Nat. Struct. Biol. 1*, 558.
Liao, M. J., Huang, K. S., & Khorana, H. G. (1984) *J. Biol. Chem. 259*, 4200.
Ludlam, C. F. C., Sonar, S., Lee, C.-P., Coleman, M., Herzfeld, J., RajBhandary, U. L., & Rothschild, K. J. (1995) *Biochemistry 34*, 2.
Mao, D., & Wallace, B. A. (1984) *Biochemistry 23*, 2667.
Miranker, A., Radford, S. E., Karplus, M., & Dobson, C. M. (1991) *Nature 349*, 633.
Miranker, A., Robinson, C. V., Radford, S. E., & Dobson, C. M. (1996) *FASEB J. 10*, 93.
Nabedryk, E., & Breton, J. (1981) *Biochim. Biophys. Acta 635*, 515.
Nabedryk, E., Gingold, M. P., & Breton, J. (1982) *Biophys. J. 38*, 243.
Nabedryk, E., Garavito, R. M., & Breton, J. (1988) *Biophys. J. 53*, 671.
Nevskaya, N. A., & Chirgadze, Y. N. (1976) *Biopolymers 15*, 637.
Ora, A., & Helenius, A. (1995) *J. Biol. Chem. 270*, 26060.
Osborne, H. B., & Nabedryk-Viala, E. (1978) *Eur. J. Biochem. 89*, 81.
Popot, J. L., & Engelman, D. M. (1990) *Biochemistry 29*, 4031.
Popot, J. L., Trewhella, J., & Engelman, D. M. (1986) *EMBO J. 5*, 3039.
Popot, J. L., Gerchman, S. E., & Engelman, D. M. (1987) *J. Mol. Biol. 198*, 655.
Prestrelski, S. J., & Arakawa, T. (1991) *Protein Eng. 4*, 739.
Provencher, S. W., & Glockner, J. (1981) *Biochemistry 20*, 33.
Ptitsyn, O. B. (1995) *Adv. Protein Chem. 47*, 83.
Rath, P., Bousché, O., Merrill, A. R., Cramer, W. A., & Rothschild, K. J. (1991) *Biophys. J. 59*, 516.
Rietveld, A., Jordi, W., & de Kruijff, B. (1986) *J. Biol. Chem. 261*, 3846.
Roder, H. (1989) *Methods Enzymol. 176*, 446.
Rothschild, K. J., & Clark, N. A. (1979a) *Biophys. J. 25*, 473.
Rothschild, K. J., & Clark, N. A. (1979b) *Science 204*, 311.
Rothschild, K. J., Braiman, M. S., Mogi, T., Stern, L. J., & Khorana, H. G. (1989) *FEBS Lett. 250*, 448.
Sahin-Toth, M., Kaback, H. R., & Friedlander, M. (1996) *Biochemistry 35*, 2016.
Sami, M., & Dempsey, C. (1988) *FEBS Lett. 240*, 211.
Schmid, F. X. (1995) *Curr. Biol. 5*, 993.
Senak, L., Davies, M. A., & Mendelsohn, R. (1991) *J. Phys. Chem. 95*, 2565.
Senko, M. W., & McLafferty, F. W. (1994) *Annu. Rev. Biophys. Biomol. Struct. 23*, 763.
Stein, R. L. (1993) *Adv. Protein Chem. 44*, 1.
Surrey, T., & Jahnig, F. (1992) *Proc. Natl. Acad. Sci. U.S.A. 89*, 7457.
Suzuki, E. (1967) *Spectrochim. Acta 23A*, 2303.
Todd, M. J., Lorimer, G. H., & Thirumalai, D. (1996) *Proc. Natl. Acad. Sci. U.S.A. 93*, 4030.
Van Zoelen, E. J., van Dijck, P. W., de Kruijff, B., Verkleij, A. J., & van Deenen, L. L. (1978) *Biochim. Biophys. Acta 514*, 9.
von Heijne, G. (1980) *Eur. J. Biochem. 103*, 431.
von Heijne, G. (1994) *Annu. Rev. Biophys. Biomol. Struct. 23*, 167.
von Heijne, G., & Blomberg, C. (1979) *Eur. J. Biochem. 97*, 175.
White, S. H., & Wimley, W. C. (1996) *Curr. Opin. Struct. Biol. 4*, 79.
Whittaker, R. G., Manthey, M. K., Le Brocque, D. S., & Hayes, P. J. (1994) *Anal. Biochem. 220*, 238.
Wickner, W. (1980) *Science 210*, 861.
Zaccaï, G., Büldt, G., Seelig, A., & Seelig, J. (1979) *J. Mol. Biol. 134*, 693.
Zhang, Y. P., Ruthven, N. A., Lewis, N. A. H., Hodges, R. S., & McElhaney, R. N. (1992) *Biochemistry 31*, 11572.

BI970146J